

8-2022

Evaluation of Single Phase Smart PV Inverter Functions in Unbalanced Residential Distribution Systems

Darren Symonette
University of Arkansas, Fayetteville

Follow this and additional works at: <https://scholarworks.uark.edu/etd>



Part of the [Electrical and Electronics Commons](#), [Power and Energy Commons](#), and the [VLSI and Circuits, Embedded and Hardware Systems Commons](#)

Citation

Symonette, D. (2022). Evaluation of Single Phase Smart PV Inverter Functions in Unbalanced Residential Distribution Systems. *Graduate Theses and Dissertations* Retrieved from <https://scholarworks.uark.edu/etd/4642>

This Thesis is brought to you for free and open access by ScholarWorks@UARK. It has been accepted for inclusion in Graduate Theses and Dissertations by an authorized administrator of ScholarWorks@UARK. For more information, please contact scholar@uark.edu.

Evaluation of Single-Phase Smart PV Inverter Functions in Unbalanced Residential Distribution Systems

A thesis submitted in partial fulfillment
of the requirements for the degree of
Master of Science in Electrical Engineering

by

Darren Symonette
University of Arkansas
Bachelor of Science in Electrical Engineering, 2020

August 2022
University of Arkansas

This thesis is approved for recommendation to the Graduate Council

Juan Carlos Balda Ph.D.
Thesis Director

Yue Zhao, Ph.D.
Committee Member

Roy McCann, Ph.D.
Committee Member

ABSTRACT

In the United States, smart PV inverters integrated with residential distribution systems are becoming a more common occurrence. With integration of smart PV inverters, power utilities are experiencing an increase of number of operations with regards to switched capacitor banks, voltage regulators and on load tap changers. These increases can lead to excess wear and tear on the devices causing power utilities to perform unwanted replacement and maintenance. However, smart PV inverters when controlled under specific functions can enable these inverters to provide reactive power and voltage control which in turn lowers the number of operations for switched capacitor banks, voltage regulators and on load tap changers. Furthermore, the standard basis is that when implementing Unbalanced Residential Distribution Systems into the grid, centralized control is a well-known choice, however, decentralized control provides a strong case for usage when using smart PV inverters in residential distribution systems.

The objective of this thesis is to provide a better understanding of Unbalanced Residential Distribution Systems tied into the distribution side of the power grid when using control functions. Furthermore, better understand and prove the theory of using decentralize control for smart PV inverters in a residential distribution system. The future work will be analyzing the role of restoration practices and islanded mode with control algorithms that are used in grid connected mode. The specific areas below will be discussed in this thesis

ACKNOWLEDGEMENTS

I would like to thank Dr. Balda for all the support and guidance throughout my MSEE Career. I would also like to thank Dr. McCann and Dr. Zhao for the technical knowledge they have provided through lectures. I also want to thank GRAPES for funding my MSEE degree.

TABLE OF CONTENTS

CHAPTER 1

INTRODUCTION	1
1.1 Motivations for this Research Work	1
1.2 Smart PV Inverters with Decentralized Control	2
1.3 Smart PV inverter functions.....	3
1.3.1 Volt/VAr Function	3
1.3.2 Fixed Power Factor Function.....	4
1.3.3 Dynamic reactive current function.....	4
1.4 Objectives of Thesis	5
1.5 Organization of Thesis	6
1.6 References.....	6

CHAPTER 2

THEORETICAL FRAMEWORK FOR ANALYSIS OF DISTRIBUTED GENERATION	8
2.1 Introduction.....	8
2.2 Quasi Static Time Series Analysis	8
2.3 EPRI OpenDSS TM	11
2.3.1 Modeling the infinite bus	12

2.3.2	Modeling distribution feeder.....	14
2.3.3	Load Modeling.....	17
2.3.4	Power factor correction and capacitor bank placement	20
2.3.5	Single-phase inverter modeling in OpenDSS™.....	21
2.4	Selected Case Studies.....	22
2.4.1	IEEE 37-bus system.....	22
2.4.2	Utility distribution feeder.....	23
2.5	Conservation Voltage Reduction	24
2.6	Integrated Volt-VAr control	24
2.7	CVR and IVVC Satisfying ANSI C84.1 Requirements	24
2.8	Conclusions.....	27
2.9	References.....	27
 CHAPTER 3		
SIMULATION PROCESS AND RESULTS		
3.1	Introduction.....	29
3.2	Implementation of Smart PV Inverter Functions in OpenDSS™.....	29
3.2.1	Implementing the Fixed Power Factor function in OpenDSS™	32
3.2.2	Implementing the Volt/VAr function in OpenDSS™.....	34

3.2.3	Implementing the Dynamic Reactive Current function in OpenDSS™.....	35
3.3	Simulation results under Different PV penetration levels	36
3.3.1	Volt/VAr function results with CVR/IVVC	38
3.3.2	Dynamic Reactive Current function results with CVR/IVVC.....	39
3.3.3	Fixed Power Factor function results with CVR/IVVC	40
3.4	Conclusions.....	41
3.5	References.....	41

CHAPTER 4

	UTILITY FEEDER 1 AND UTILITY FEEDER 2 CASE STUDIES IN TYPHOON HIL.....	43
4.1	Introduction.....	43
4.2	Typhoon HIL Summarized Description.....	43
4.2.1	Modeling the infinite the bus	44
4.2.2	Modeling distribution feeder.....	45
4.2.3	Load modeling	46
4.2.4	Power Factor Correction and capacitor bank placement	47
4.3	Selected Distribution Feeders	48
4.3.1	Utility feeder 1	48
4.3.2	Utility feeder 2	49

4.4	Conclusions.....	50
4.5	References.....	51

CHAPTER 5

	CONCLUSIONS AND FUTURE WORK.....	52
5.1	Conclusions.....	52
5.2	Recommendations for future work	53
5.2.1	PHIL co-simulation architecture.....	53
5.2.2	Role of single-phase smart PV inverters in supporting URDS restoration practices.....	54
5.2.3	Evaluation of Islanded operations for unbalance residential distribution systems	55
5.3	References.....	55

APPENDIX A

	OPENDSS™ AND MATLAB SCRIPTS	56
A.1	MATLAB main.m File	56
A.2	OpenDSS™ Line Codes and Table A.5.....	59
A.3	Load model script	61
A.4	OpenDSS™ Capacitor bank models.....	62
A.5	Single-phase PV Inverter code.....	63
A.6	Reference	66

APPENDIX B

TYPHOON HIL INITIALIZATION SCRIPTS67

B.1 Typhoon HIL initialization scripts 67

B.2 Pre-built Scada Panel72

LIST OF FIGURES

Figure 1-1 Simplified block diagram of the entire PV system and inverter control	3
Figure 1-2 Volt/VAr function at the PCC	4
Figure 1-3 Dynamic Reactive Current function at the PCC	5
Figure 2-1 QSTS Algorithm implementation	9
Figure 2-2 Load dynamics over a 14-day period	10
Figure 2-3 Solar irradiance over a 14-day period	11
Figure 2-4 MATLAB/OpenDSS™ Simulation Platform	11
Figure 2-5 Modified IEEE 37-bus system in OpenDSS™	12
Figure 2-6 Infinite bus model diagram.....	13
Figure 2-7 Infinite bus model diagram with transformer impedance.....	14
Figure 2-8 Nominal π equivalent circuit	14
Figure 2-9 Overhead pole layout for distribution circuit configuration.....	16
Figure 2-10 Schematic of primary feeder with loads.....	18
Figure 2-11 Power triangle concept for PFC	21
Figure 2-12 OpenDSS™ capacitor object code	21
Figure 2-13 Utility feeder	23
Figure 2-14 Modified IEEE 37-bus system voltage profile for No PV penetration case.....	25
Figure 2-15 Modified IEEE 37-bus system voltage profile for 20% PV penetration case	25
Figure 2-16 Modified IEEE 37-bus system voltage profile for 40% PV penetration case	26
Figure 2-17 Modified IEEE 37-bus system voltage profile for 60% PV penetration case	26
Figure 3-1 Solar irradiance over a 14-day period	30

Figure 3-2 Phase A for PV system at bus 701 with a 0.95 leading power factor.....	32
Figure 3-3 Open-DSS Volt/VAr function.....	32
Figure 3-4 Open-DSS Dynamic reactive current function.....	32
Figure 3-5 PV system performing the FPF function for 60% PV penetration.....	34
Figure 3-6 PV system performing the VV function for 60% PV penetration.....	35
Figure 3-7 PV system performing DRC function for 60% PV penetration	35
Figure 3-8 OLTC operations for the VV function at 60% PV Penetration for the modified IEEE 37-bus system.....	38
Figure 3-9 OLTC operations for the VV function at 60% PV Penetration for Utility feeder.....	38
Figure 3-10 OLTC operations for the DRC function at 60% PV penetration for the modified IEEE 37-bus system.....	39
Figure 3-11 OLTC operations for the DRC function at 60% PV penetration for Utility feeder...	39
Figure 3-12 OLTC operations for the FPF function at 60% PV penetration for modified IEEE 37-bus system.....	40
Figure 3-13 OLTC operations for the FPF function at 60% PV penetration for Utility feeder	40
Figure 4-1 Pre-built SCADA initialization panel in Typhoon HIL.....	44
Figure 4-2 Three-phase voltage source representing infinite the bus in Typhoon HIL.....	45
Figure 4-3 Transmission line segments graphic in Typhoon HIL.....	45
Figure 4-4 Schematic of load model in Typhoon HIL.....	46
Figure 4-5 Three phase load component and parameters.....	47
Figure 4-6 Schematic of capacitor bank layout in Typhoon HIL.....	47
Figure 4-7 Utility feeder 1 Typhoon HIL model.....	48
Figure 4-8 Utility feeder 1 voltage profile.....	49
Figure 4-9 Utility feeder 2 Typhoon HIL model.....	49

Figure 4-10 Utility feeder 2 voltage profile.....	50
Figure 5-1 FLISR scenario for modified IEEE 37-bus system.....	54

LIST OF TABLES

Table. 2-1 Resistance and reactance in Ohms for the modified IEEE 37-bus system	17
Table. 2-2 Utility feeder summary	23
Table 3-1 Effects of CVR/IVVC with Fixed Power Factor function (0.95 leading)	33
Table 3-2 Effects of smart PV inverter functions on OLTC for different PV penetration scenarios for the modified IEEE 37-bus system and Utility feeder	36
Table 3-3 Effects of smart PV inverter functions on SCBs for different PV penetration scenarios on the modified IEEE 37-bus system.....	37
Table 4-1 Utility feeder 2 main characteristics	50
Table A.5 for primary feeder sizing	60

CHAPTER 1

INTRODUCTION

1.1 Motivation for this Research Work

In the power utility industry, distributed generation (DG) is becoming a more prevalent source, particularly in the form of rooftop single-phase PV smart inverters. This rise of rooftop solar can affect of the voltage at the point of common coupling (PCC) or interconnection points. PV inverters connected at the end of a distribution feeder can have greater impacts on the line voltage. Furthermore, depending on the PV penetration capacity and the PCC location, unwanted voltage rises may occur rising above the ANSI C84.1 upper limit [1]. In addition, erratic weather patterns can cause instabilities in PV generation causing unwanted voltage fluctuations. These rapid changes and fluctuations can increase the number of operations for voltage regulators (VR), on load tap changing (OLTC) transformers and switched capacitor banks (SCB) when placed in high PV penetration scenarios leading to increased maintenance costs for power utilities [1-3]. Reference [2] indicates that VR operations may increase by an average of 72% with the addition of DG. To address these issues, utilities can use mitigation techniques by using a variety of centralized and decentralized methods using PV inverter functions. PV smart inverters are implemented into the grid with smart functions applied to assist in reactive power and voltage support [4]. The availability of single-phase PV inverters thus presents an opportunity to evaluate if decentralize control of single-phase rooftop solar arrays may overcome the above disadvantages of DG. The use of decentralize control for solar PV inverters are beneficial from a computational standpoint. The time taken for a decentralized controller to compute an optimal solution and the dynamics of a distribution system must be considered. The state of a distribution system changes

every second due to changes in residential loads and varying solar irradiation. In an advanced distribution management system (ADMS) performing centralized control, time lags occur with regards to devices in the distribution system and the network [5]. However, from a decentralized control aspect, time lags and microgrid communication delays are less intense establishing a quicker response time for grid optimization.

1.2 Smart PV Inverters with Decentralized Control

PV inverters are traditionally used to inject active power into the PCC at unity power factor. As previously stated, the single-phase PV inverters are evaluated from a decentralized control in an attempt to not only reduce communication delays but also prevent against cyber-attacks occurring at a centralized controller.

Decentralization may enable a more robust distribution system against cyber-attacks because the single-phase PV inverters do not need to connect to a centralized point since they can operate independently of each other. Fig. 1-1 illustrates a simplified block diagram of the PV model and its connection to the grid. Through this representation, a decentralized control approach is addressed by implementing the desired control function into each inverter operating independently of each other without the need for an ADMS or centralized controller. Therefore, each smart PV inverter operates by performing a selected function to provide grid support such as reactive power control, voltage regulation, frequency support or ride through applications. The specific functions selected for consideration in this thesis are the Volt/VAr, Fixed Power Factor, and Dynamic Reactive Current (DRC).

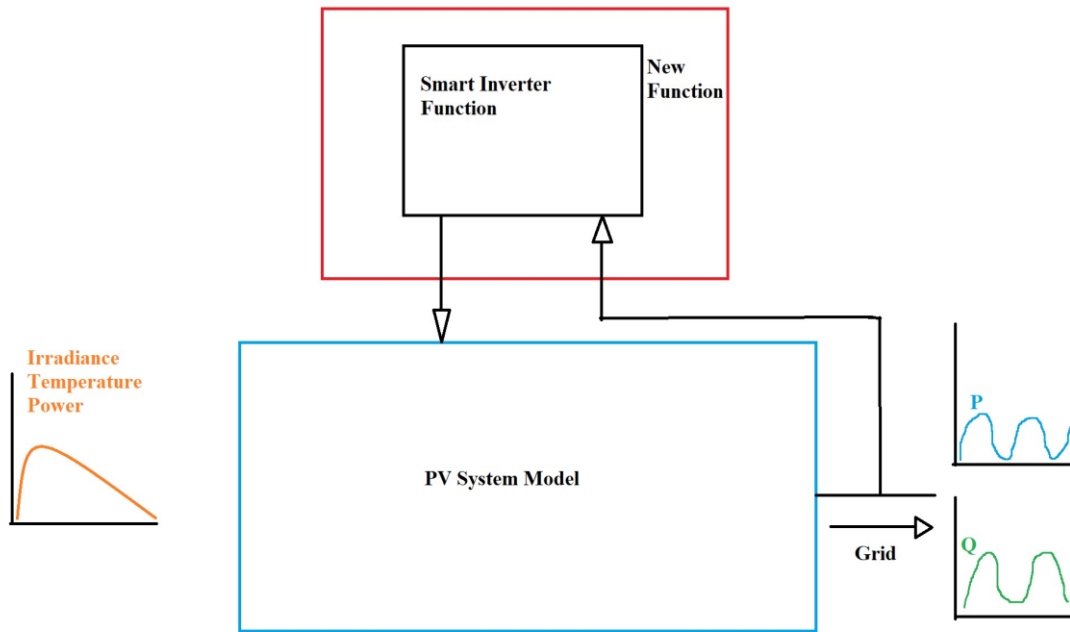


Fig. 1-1 Simplified block diagram of the entire PV system and inverter control

1.3 Smart PV Inverter Functions

Smart PV inverters possess the ability to perform different functions at the PCC in a distribution system. Many power utilities throughout the United States are beginning to understand the benefits of these functions with regards to reactive power, voltage, and frequency control [6]. For the selected case studies, the Volt/VAr, Fixed Power Factor and Dynamic Reactive Current function (DRC) are selected to study the smart PV inverter effects under high PV penetration scenarios.

1.3.1 Volt/VAr function

The objective of the Volt/VAr function is to provide reactive power output in its own response to the voltage at the PCC or local service voltage [4] as illustrated in Fig. 1-2.

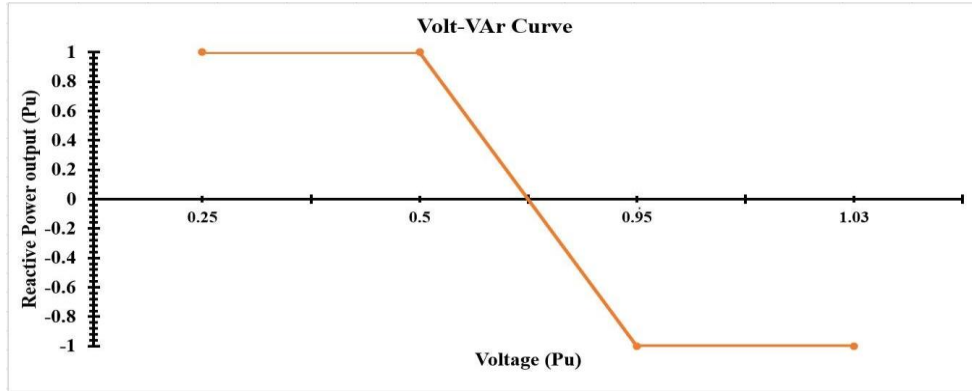


Fig. 1-2 Volt/VAr function at the PCC

Based on the PCC voltage, the inverter determines the amount of reactive power to be injected based on the inverter reactive power capability. The Volt/VAr function contains a piecewise linear curve of the desired Volt/VAr behavior. Its behavior is based on how its programmed to better provide grid support depending on the conditions at the PCC and within the distribution system.

1.3.2 Fixed power factor function

This function operates the PV inverter at a fixed power factor regardless of its output power. In OpenDSS™, DG patterns over a period can be implemented in a Quasi-Static Time Series (QSTS). As the inverter output changes, this function changes the reactive power with regards to the set power factor based on the active power output [2].

1.3.3 Dynamic reactive current function

This function operates like the Volt/VAr function; however, dissimilarities are that it provides dynamic reactive current support at the PCC in response to voltage variations [1]. Fig. 1-3 illustrates the DRC support concept and the ability to provide dynamic reactive current on a percentage basis at the PCC.

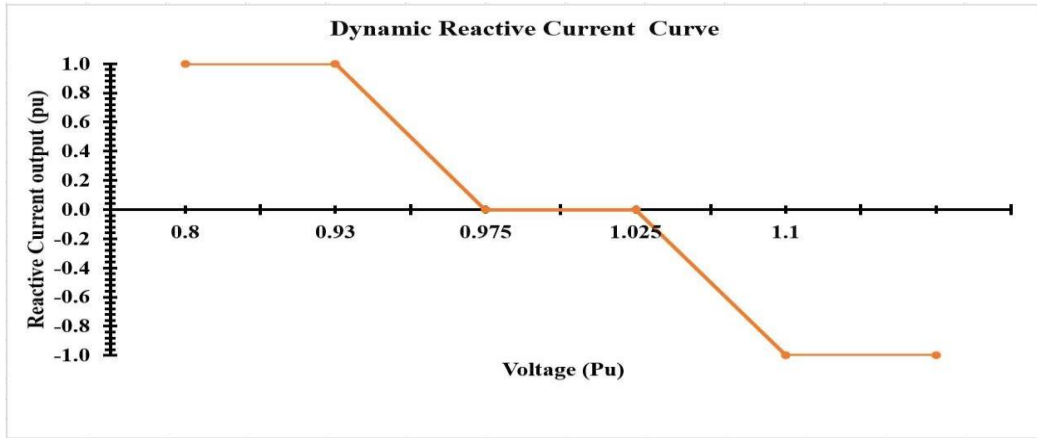


Fig. 1-3 Dynamic Reactive Current function at the PCC

1.4 Objective of the Thesis

The main objective of this thesis is to evaluate the impact of different levels of rooftop single-phase PV inverters, particularly those equipped with smart functions, in Unbalanced Residential Distribution Systems (URDS) from a decentralized control aspect. This will be done in the following 4 steps:

1. Selecting the proper software package to address modeling of both loads, and distributed generation varying with time of the day. Traditional power flow tools are not able to conduct a QSTS analysis so it must be ensured that a capable software package is selected to accommodate for the time variations of the loads and generation.
2. Applying Conservation Voltage Reduction (CVR) and integrated Volt/VAR Control (IVVC) to the control of the distribution system.
3. Selecting the case studies that could be considered representatives of typical URDS.

4. Selecting the smart PV inverter functions more suitable for the selected case studies.

1.5 Organization of the Thesis

The theory behind the analysis of DG will be presented in Chapter 2 that will comprise the complete design process for the selected case studies and DG. The simulation process and results for each smart PV inverter function for selected PV penetration scenarios for both case studies will be presented in Chapter 3. It also will include the implementation process in Typhoon HIL for the smart PV inverter functions in the selected case studies under CVR and IVVC will be addressed in Chapter 4 to verify the OpenDSS/MATLAB results. The conclusions and recommendations for future work will be given in Chapter 5.

1.6 References

1. Hariri, M. O. Faruque, R. Soman and R. Meeker, "Impacts and interactions of voltage regulators on distribution networks with high PV penetration," *2015 North American Power Symposium (NAPS)*, 2015, pp. 1-6, doi: 10.1109/NAPS.2015.7335212.
2. D. Symonette and J. C. Balda, "Evaluation of Single-Phase PV Smart Inverter Functions in Unbalanced Residential Distribution Systems," *2021 IEEE 12th International Symposium on Power Electronics for Distributed Generation Systems (PEDG)*, 2021, pp. 1-6, doi:
3. K. Alboaouh and S. Mohagheghi, "Impact of Rooftop Photovoltaics on the Distribution System," *Journal of Renewable Energy*, 2020. 1- 23. 10.1155/2020/4831434
4. Smart Grid Ready PV Inverters with Utility Communication: Results from Field Demonstrations, EPRI Report 3002008557, May 2016.
5. Phan-Tan, Chi-Thang, and Martin Hill. 2021. "Decentralized Optimal Control for Photovoltaic Systems Using Prediction in the Distribution Systems" *Energies* 14, no. 13: 3973. <https://doi.org/10.3390/en14133973>

6. R. C. Dugan, The Open Distribution System Simulator (OpenDSS), Electric Power Research Institute, Palo Alto, CA, USA, 2019.

CHAPTER 2

THEORETICAL FRAMEWORK FOR ANALYSIS OF DISTRIBUTED GENERATION

2.1 Introduction

The objective of this chapter is to present the theoretical framework for evaluating distribution systems with high percentages of distribution generation (DG). Hence, this chapter begins with selecting the appropriate software tools for considering the time variation of DG. Most power system analysis software's perform snapshot analysis that investigate specific time periods. A snapshot analysis is not well suited for DG analysis because it is not able to analyze the overall impact of DG from a geographical standpoint and the chronological diversity of DG output behavior. While analyzing suitable algorithms for the following case studies, a Quasi-Static Time Series Analysis (QSTS) is a technique well suited to capture time-dependent aspects in a power flow. This chapter presents the selected case studies and the modeling of a distribution feeder in EPRI OpenDSSTM. Lastly, the control approaches based on the selected control strategies based on Integrated Volt/VAr Control (IVVC) and Conservation Voltage Reduction (CVR) are illustrated.

2.2 Quasi Static Time Series Analysis

QSTS is used in this thesis to study power systems with loads and DG varying over a 14-day period. As previously stated, QSTS has the capability to meticulously analyze the behavioral patterns of a distribution system having DG whose generation outputs vary with time [1]. QSTS simulations are solved by conducting a sequential steady-state power solution in a rapidly

processing manner. In other words, a QSTS analysis gives a discrete model that allows time dependent states to be captured at specific points in time. As an alternative of providing a snapshot analysis of the worst-case scenario in a distribution system. The converging state of each iteration is used as the beginning state of the next one; therefore, it is ensured that the appropriate simulation step time along with the implemented load shape is selected. By selecting an appropriate step time based on the period of which the QSTS study is conducted, the amount of sequential power flow solutions can be extremely high causing the QSTS to become computationally cumbersome. Therefore, power flow solution values can be reduced by using efficient algorithms.

Fig. 2-1 illustrates the flowchart for the QSTS algorithm used for this study. The circuit compilation begins with the circuit model where the time step and time-period of study or time horizon are determined.

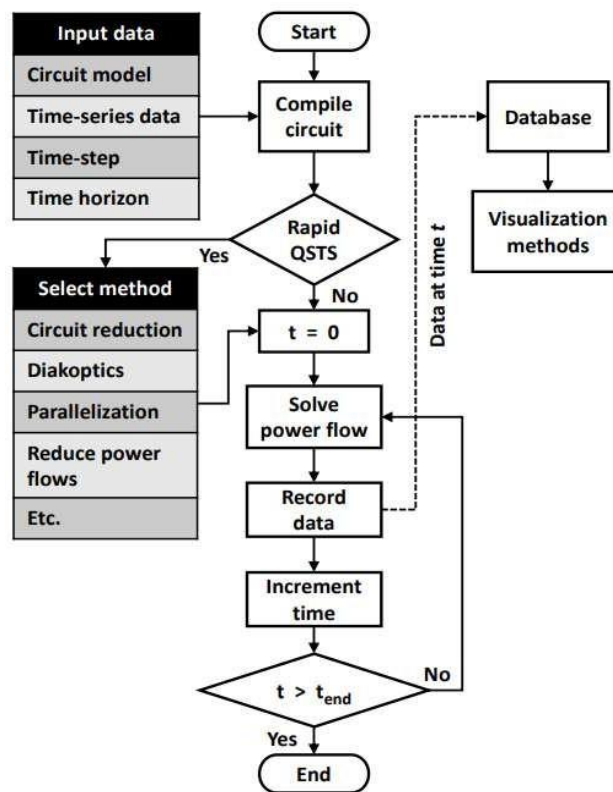


Fig. 2-1 QSTS algorithm implementation [2]

If the rapid QSTS option is selected the circuit model is reduced to where an optimization method is selected and the rapid QSTS is conducted. However, if a rapid QSTS is not selected a standard power flow is performed. The QSTS algorithm is executed over the time period and the data is recorded and sent to a database to determine appropriate visualization methods. After the QSTS simulation is completed, the task of analyzing the power flow results to under the effects of DG control strategies is performed. Furthermore, the QSTS operates along with the desired mode determined in the appropriate distribution software package that must possess the capability to obtain load flow solutions with the integration of a load shapes for DG output and consumer loads [3]. For the loads, the selected load shape functions as a load multiplier that multiplies the maximum apparent power of the system between 1 and 0 based on the load shape at a particular point in the determined time as shown in Fig. 2-2. The mode for this case study was the daily function because the QSTS simulation occurred over 14 days. The load shape was implemented into the “main.m” MATLAB script which contains the QSTS algorithm given in Appendix A. Fig. 2-3 displays the PV output of the PV inverters over 14 days which affects the output apparent power by multiplying the PV load shape by its output power [4]. Fig. 2-2 and Fig. 2-3 are the input data implemented in the circuit compilation in the QSTS algorithm.

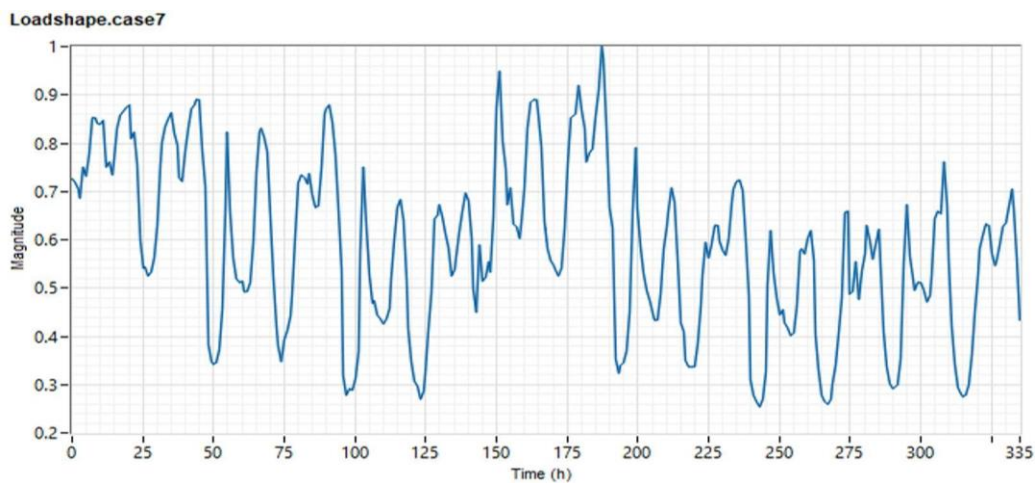


Fig. 2-2 Load dynamics over a 14-day period

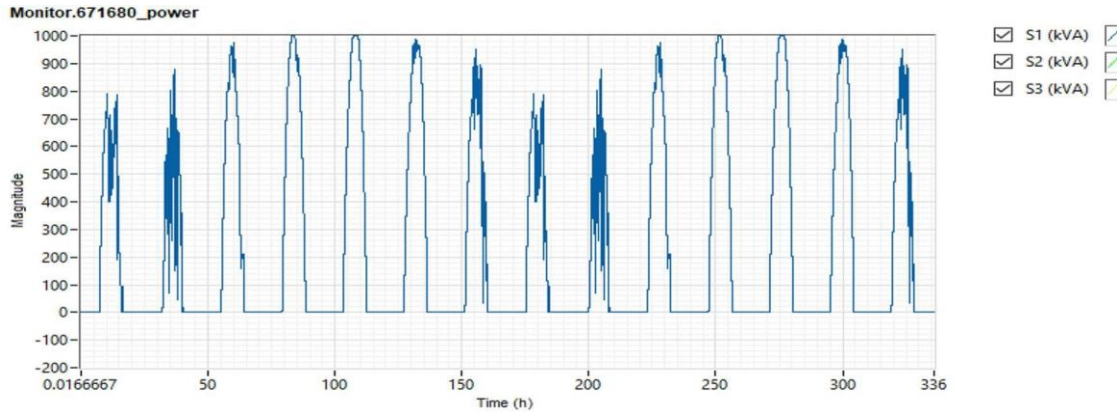


Fig. 2-3 Solar irradiance over a 14-day period

2.3 EPRI OpenDSS™

EPRI OpenDSS™ is the software package used to analyze the selected case studies. The reasoning for using OpenDSS™ is that it has the capabilities to perform QSTS load flow studies with distribution energy resources (DER) in unbalanced scenarios. The OpenDSS™ program is an open-source electric power distribution system simulator that specializes in the application of distribution resource integration and grid modernization [3]. Fig. 2-4 illustrates the MATLAB/OpenDSS™ simulation platform connection.

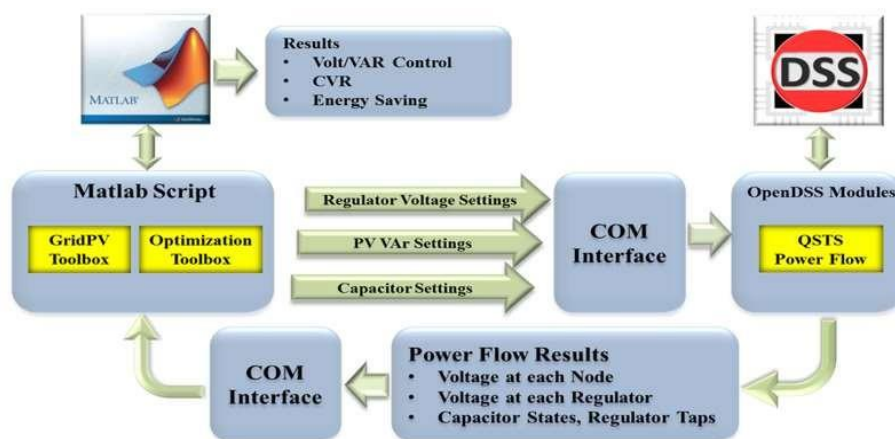


Fig. 2-4 MATLAB/OpenDSS simulation platform

EPRI OpenDSS™ is interfaced with MATLAB to perform grid optimization using MATLAB scripts and provide a detailed status update of the capacitor banks, voltage regulators, node voltages and (DG) in the distribution system. A QSTS power flow is performed in OpenDSS™, and the power flow results are transferred to MATLAB via the COM interface. The results are analyzed in MATLAB where grid control and optimization methods are implemented and applied to OpenDSS™ using the COM interface. For the MATLAB/OpenDSS™ simulation platform to operate, a COM interface between the two software platforms must be established. The COM interface allows the users to design and execute custom solution modes and access features from external programs [7].

2.3.1 Modeling the infinite bus

The infinite bus is modeled by an ideal voltage source and a series impedance. The modified IEEE 37-bus system shown in Fig. 2-5 was modeled with a three-phase voltage regulator in front of the substation transformer to represent the On Load Tap Changer (OLTC) in which its operation under high PV penetration scenarios will be analyzed.

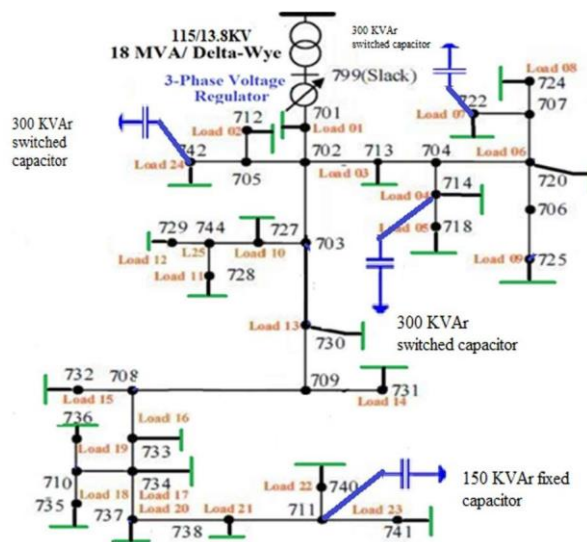


Fig. 2-5 Modified IEEE 37-bus system in OpenDSS™ [4]

The dynamic load curve shown in Fig. 2-2 and the solar irradiance displayed in Fig. 2-3 were implemented into the modified IEEE 37-bus system via OpenDSS™ and MATLAB COM interface which allows a QSTS to be performed. The modified IEEE 37-bus system infinite bus was modeled after a utility substation with a high-side voltage of 115 kV and a low-side voltage of 13.8 kV. The distribution feeder was loaded to 6.4 MW + 2.2 MVA_r with 4 capacitor banks to provide power factor correction. The infinite bus was modeled after a utility substation with a 20 MVA transformer and the secondary voltage was initially 4.16 kV_{LL} so it was converted to a line-to-line voltage of 13.8 kV. The short circuit impedance is calculated using the short-circuit power MVA_{sc} and the rated line-neutral voltage per the following relationship:

$$Z_{sc}^F = \frac{V_{LN}^2}{\frac{MVA_{sc}}{3}} \quad (1)$$

The equivalent transformer impedance in Ohms using its percentage impedance is given by:

$$Z_{eq} = \frac{Z_{snfr} V_{LL}^2}{100 MVA} \quad (2)$$

The Z_{sc} shown in Fig. 2-6 refers to the equivalent series impedance $Z_{sc} = jX_{sc}$ which is assumed to be purely inductive modeling the fact that the infinite bus is not an ideal source. Once the short-circuit impedance is determined, Z_{eq} is placed after node 2 shown in Fig. 2-7.

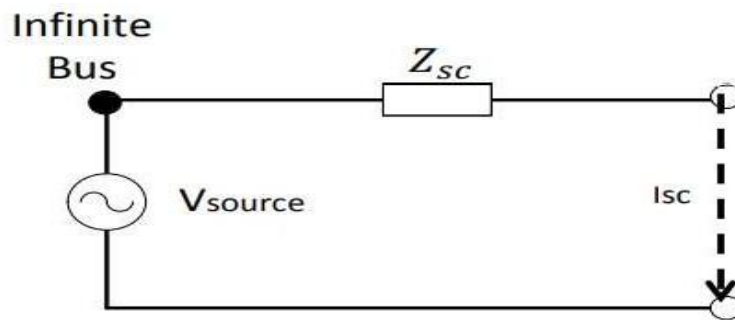


Fig. 2-6 Infinite bus model diagram [5]

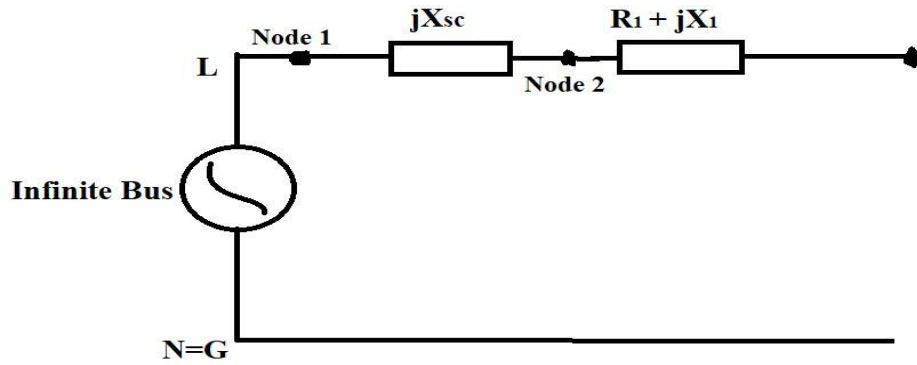


Fig. 2-7 Infinite bus model diagram with transformer impedance [5]

2.3.2 Modeling distribution feeders

Line objects are used to model multi-phase two-port lines and cables. The π model with a shunt capacitance illustrated in Fig. 2-8 is used to model the respective lines in the selected case studies. OpenDSS defines line objects as power delivery elements which are described based on their impedances based on matrix values. Line codes are essentially series impedances matrices and nodal capacitance admittance matrices for line and cables [7]. The selected case studies were modeled in OpenDSSTM by building line configurations which are placed in line codes to configure the particular distribution feeder. By creating a line code, a line can be established by its line code and length.

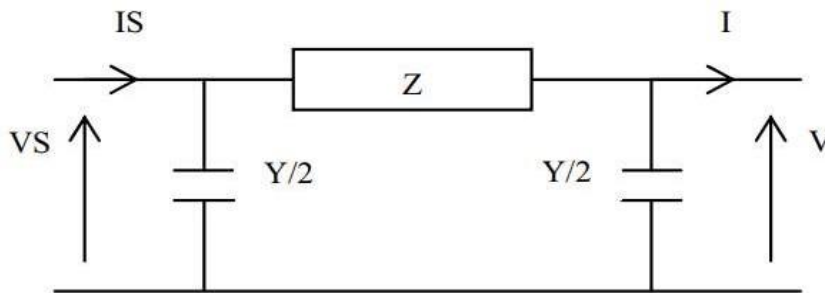


Fig. 2-8 Nominal π equivalent circuit [6]

In OpenDSS™, each line has the capability to be modeled individually or can be modeled as a previously used line using line codes. The benefit of using line codes is that when designing the impedance segments for a distribution feeder, it prevents the user from having to produce an additional set of impedance matrices into a new line which can establish a more efficient modeling process. If multiple segments share the same characteristics the same line code can be used for those lines. The line codes defined in OpenDSS™ are given in Appendix A. When generating a line code, the following properties are considered:

- Nphases — The number of phases.
- BaseFreq — The frequency value for the distribution system e.g. (60 or 50 Hz)
- Rmatrix — The series resistance matrix.
- Xmatrix — The series reactance matrix
- Cmatrix — The shunt nodal capacitance matrix.

For design considerations of primary feeders, the rated current must be determined to select the proper conductor. Furthermore, factors such as load forecasting, power losses, voltage drops, transformer rating and load growth rate are also considered [5]. The rated current was calculated as follows.

$$I_{\text{rated}} = \frac{S_{3\text{phase}}}{\sqrt{3}V_{LL}} \quad (3)$$

The rated current of the transformer considers a safety margin to select the proper feeder conductor size. The desired conductor size for the primary feeder is selected from Table A.5 [5] shown in Appendix A. Once the AWG rating is selected, the pole configuration illustrated in Fig.

2-9 is used to calculate the positive sequence impedance for the primary feeder. D_{ab} , D_{bc} , D_{ac} units of measurements are in inches, so they are converted to feet where the spacing factor for the phases was calculated using the following [5]:

$$d_p = \sqrt[3]{D_{ab} D_{bc} D_{ac}} \quad (4)$$

$$X_{dp} = 0.05292 \log_{10} d_p \quad (5)$$

Using the numerical values from (4) and (5), (6) are implemented calculating the in Ω/mile each segment impedance which is presented in Table. 2-1 for the modified IEEE 37-bus system.

$$Z_1 = Z_2 = r_{ap} + j(X_{ap} + X_{dp}) \quad \Omega/\text{mile} \quad (6)$$

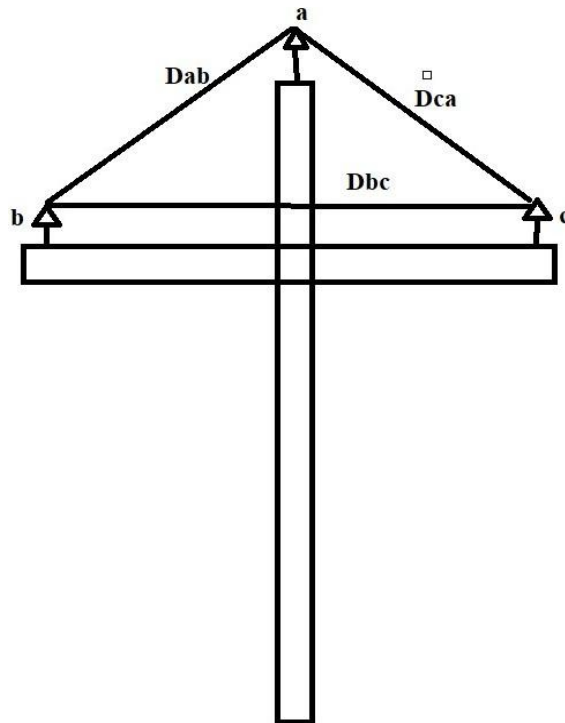


Fig. 2-9 Assumed overhead pole circuit configuration

Table. 2-1 Resistance and reactance in Ohms for the modified IEEE 37-bus system

Segments	R _{ap}	j (X _{ap} + X _{dp})
1	0.34595	1.11
2	0.17952	0.576
3	0.0748	0.24
4	0.06732	0.216
5	0.24684	0.792
6	0.04488	0.144
7	0.1122	0.36
8	0.01496	0.048
9	0.1496	0.48
10	0.05984	0.192
11	0.04488	0.144
12	0.05236	0.168
13	0.14212	0.456
14	0.02244	0.072
15	0.05984	0.192
16	0.05984	0.192
17	0.1122	0.36
18	0.05984	0.192
19	0.0374	0.12
20	0.23936	0.768
21	0.0748	0.24
22	0.0374	0.12
23	0.09724	0.312
24	0.09724	0.312
25	0.17204	0.552
26	0.1122	0.36
27	0.05236	0.168
28	0.0374	0.12
29	0.10472	0.336
30	0.11968	0.384
31	0.09724	0.312
32	0.0748	0.24
33	0.0748	0.24
34	0.0374	0.12
36	0.05236	0.168

2.3.3 Load modeling

Once the primary feeder is designed, the system loads are modeled by considering two specific elements: Rload representing the active power in the bus, and Xload the reactive power considered as an inductor [6] and modeled along the feeder as shown in Fig. 2-10. The loads were modeled as follows.

These two representations specify an individual load whether single, two or three phases.

$$R_{load} = \frac{V_{LL}^2}{P_{3\phi}} \quad or \quad R_{load} = \frac{V_{LN}^2}{P_{\phi}} \quad (7)$$

$$X_{load} = \frac{V_{LL}^2}{Q_{3\phi}} \quad or \quad X_{load} = \frac{V_{LN}^2}{Q_{\phi}} \quad (8)$$

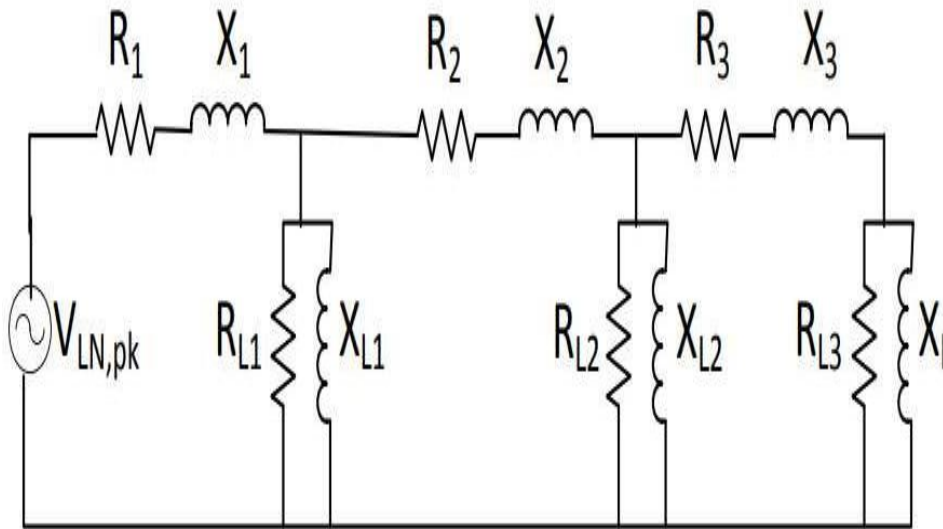


Fig. 2-10 Simplified schematic of primary feeder with loads [5]

In OpenDSS™, load objects are power conversion elements that can be multiplied and changed over a given period. Loads can fluctuate in value based on given multipliers as determined by global values in the OpenDSS™ code. These values are set over a determined amount of time which define a load shape to as daily, yearly or a duty cycle. For QSTS simulations, loads depict real life scenarios where fluctuations and load changes occur. This is because in a distributions system load demands can increase or decrease depending on the customer demands as previously shown in Fig. 2-2. When modeling loads in OpenDSS™, they can either be balanced or unbalanced, entered as three-phase or single-phase loads, and can be specified as follows:

- kW, kVAr
- kW, PF
- kVAr, PF

For the modified IEEE 37-bus system, each load is specified based on its kW and kVAR demands, number of phases, service voltage, connection and model, and bus location. The load model must also be considered which affects the variation of the loads with regards to voltage [8]. The code that was implemented for the load modeling is displayed in Appendix A.

OpenDSSTM contains 8 load models that allow loads to behave in multiple ways in terms of their relationships with the service voltage. For the modified IEEE 37-bus system, the ZIP model was selected for all loads. By using the “batchedit” function in the OpenDSS/MATLAB COM interface, the ZIP model equations below are implemented for each load:

$$P = P_o \left[Z_p \left(\frac{V_i}{V_o} + I_p \frac{V_i}{V_o} + P_p \right) \right] \quad (9)$$

$$Q = Q_o \left[Z_q \left(\frac{V_i}{V_o} + I_q \frac{V_i}{V_o} + P_q \right) \right] \quad (10)$$

The ZIP model is used to represent loads under variable conditions in a distribution system. ZIP coefficient of the load model a constant impedance, current or power. ZIP models are used to represent power consumed by a load as a function of the voltage [8]. (9) and (10) are polynomial expressions that defines the active and reactive powers of the ZIP coefficient models. P and Q are the active and reactive powers, respectively, at operating voltage V_i . P_o and Q_o represents the active and reactive powers at the rated voltage V_o . Z_p , I_p and P_p represents ZIP coefficients for the active powers and Z_q , I_q and P_q represents the ZIP coefficients for the reactive powers.

2.3.4 Power factor correction and capacitor bank placement

In a distribution system, reactive power changes due to fluctuations of the consumer loads. This determines the leading or lagging characteristics of a load and its power factor [5]. The power factor determines how efficiently electricity is being used. In real-world scenarios, the loads in a distribution system are mostly inductive by nature due to transmission lines, transformers and motor apparatus used in household, commercial consumers. A high lagging reactive power causes unwanted voltage drops along a distribution feeder which can violate ANSI C84.1 standard. Fig. 2-11 illustrates the power factor correction concept for a distribution system. As an example, the modified IEEE 37-bus system power factor was corrected by implementing three 300 kVAR switched capacitor banks for maximum load and one 150 kVAR fixed capacitor bank for minimum load that was connected to selected buses shown in Fig. 2-12. The instructions for the capacitor bank in OpenDSS™ are given in Appendix A.

Capacitor placement is a vital aspect in power loss and voltage regulation in a distribution system. To obtain the most effective locations for capacitor placement in a distribution system, a feeder voltage profile study is performed to better determine the voltage that is within the required limits [5]. Each load kW, kVAR and PF is analyzed, along with the desired power factor and feeder circuit voltage. The IEEE 37-bus system and utility feeder are relatively rural feeders, therefore, a 3V rise for the distribution feeder voltage is the maximum change in voltage that can occur when a SCB is placed into operation [5].

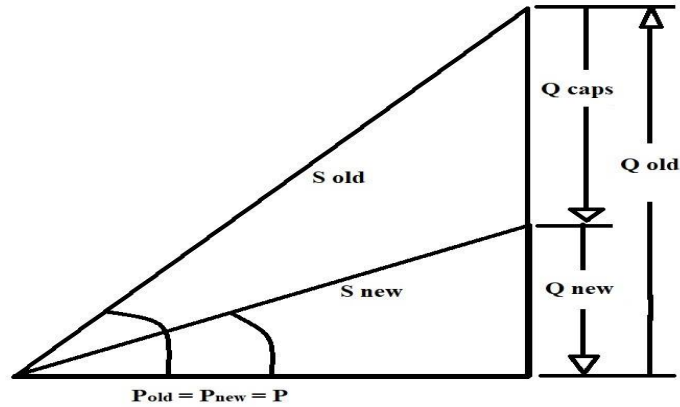


Fig. 2-11 Power triangle concept for PFC

```

!FIXED CAPACITORS
New Capacitor.C703 Bus1=711 Phases=3 Numsteps=3 kVAR=150 kV=13.8 states=[1]

!SWITCHED CAPACITORS
New Capacitor.C730 Bus1=714 Phases=3 Numsteps=3 kVAR=300 kV=13.8
New Capacitor.C711 Bus1=722 Phases=3 Numsteps=3 kVAR=300 kV=13.8
New Capacitor.C737 Bus1=742 Phases=3 Numsteps=3 kVAR=300 kV=13.8

```

Fig. 2-12 OpenDSS™ capacitor object code

2.3.5 Single-phase inverter modeling in OpenDSS™

For single-phase inverters, OpenDSS™ classifies inverters as generator objects that is, a power conversion element modeled as a negative load. Generator object ratings are defined using the nominal real power, reactive power and power factor values which are modified and changed via multipliers in a daily, yearly or duty cycle load shape. For the modified IEEE 37- bus system and utility feeder, the single-phase PV inverters were modeled to be a current injection source

using the Norton equivalent method [7]. Where, OpenDSS™ classifies them as a current-limited constant P and Q model. The single-phase PV inverter code is shown in the Appendix A.

2.4 Selected Case Studies

As explained previously, the modified IEEE 37-bus system was selected as one of the desired case studies. The IEEE 37-bus system was modified to convert it to a 13.8kV system and a QSTS study was performed under multiple high PV penetration scenarios to study capabilities of the selected smart PV functions. After analyzing selected smart PV functions under high PV penetration scenarios, a real-life utility feeder was modeled in OpenDSS™ MATLAB, and its results were compared to the modified IEEE 37-bus system.

2.4.1 IEEE 37-bus system

The initial case study was the IEEE 37-bus system which was modified to study the behavior of single-phase PV inverters. The IEEE 37-bus system contained the perfect number of buses to analyze the PV penetration at each bus. The IEEE 13-bus system and IEEE 123-bus system were initially considered but, the IEEE 13-bus system did not contain enough buses while the IEEE 123-bus system contained too large a quantity of buses to analyze. The IEEE 37-bus feeder was modeled after an actual feeder in California with a 4.8 kV operating voltage. The system is characterized by delta configuration with the substation voltage regulation being two single-phase open-delta regulators, and unbalanced spot loads. The IEEE 37-bus system is an uncommon configuration however as previously stated it was selected because its reasonable bus quantity and adapted after a utility substation for study purposes. The utility substation contained three primary distribution feeders. However, two of the distribution feeders were modeled as constant RL loads using (8) and (9) and connected to the substation.

2.4.2 Utility distribution feeder

After modeling and gathering results from the modified IEEE 37-bus system, a utility feeder shown in Fig. 2-13 was modeled in OpenDSS™. Using the load fault data given in an Excel file, the utility feeder was designed using the same process for the modified IEEE 37-bus system. A summary of the utility feeder is shown in Table. 2-2.

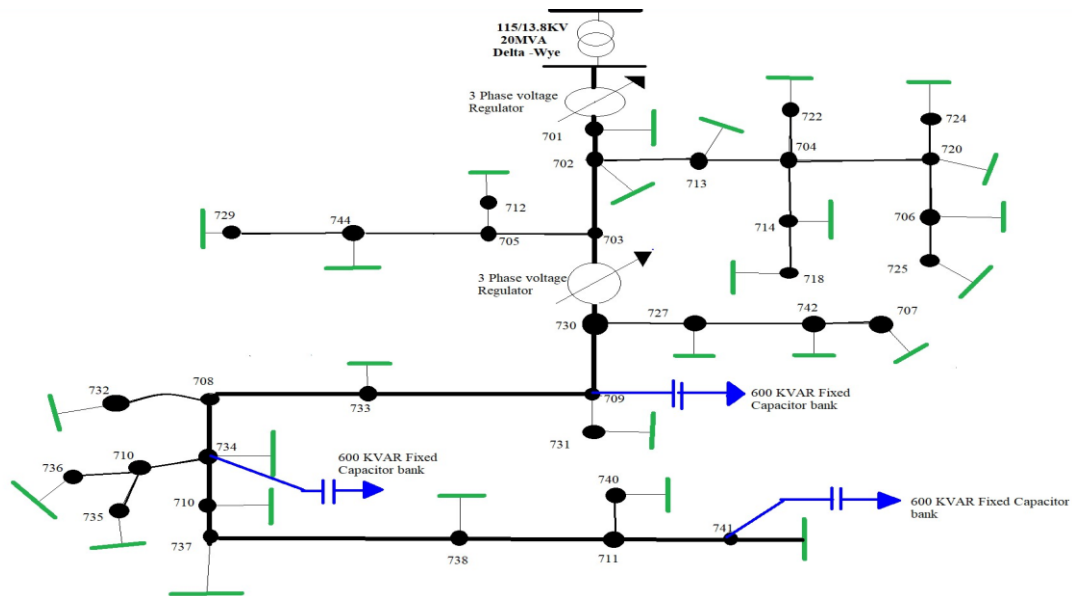


Fig. 2-13 Utility feeder

Table. 2-2 Utility feeder summary

Sub transmission voltage (kV)	115
System voltage (kV)	13.8
kW Demand (kW)	6593
kVAr Demand (kVAr)	2287
Amp Demand (A)	295
PF Demand	0.94
Service xfmr connected (MVA)	29158
No. of voltage regulators	1
No. of fixed capacitor banks	3
No. of switch capacitor banks	0

2.5 Conservation Voltage Reduction

Conservation Voltage Reduction (CVR) is a common method used by power utilities that is applied within the ANSI C84.1 standard to improve energy efficiency. By reducing the service voltage of a distribution feeder, CVR can reduce energy consumption while still satisfying the minimum 0.95 pu voltage at all buses of the feeder [9]. The ANSI C84.1 ranges from 126 -114 V but, with CVR implemented the feeder operates in the lower half voltage range; that is ,120-114V and was applied to both the modified IEEE 37-bus system and the utility feeder.

2.6 Integrated Volt-VAr Control

The integrated Volt/VAr control method was applied to the modified IEEE 37- bus system and utility feeder to provide voltage and reactive power control capabilities with no PV penetration. IVVC assist in voltage and reactive power control by allowing pieces of equipment such as OLTCs, voltage regulators (VR) and switched capacitor banks to operate in a sequential manner to provide a flat voltage profile [10].

2.7 CVR and IVVC Satisfying ANSI C84.1 Requirements

By applying CVR and IVVC, the voltage profile remains within the ANSI C84.1 standard while remaining fairly flat and satisfying the lower half voltage range as shown in Fig. 2-14 and Fig 2-15. With CVR and IVVC implemented simultaneously, the number of operations for the OLTC and switched capacitor banks for both distribution systems for the “No PV” case decreases. Fig 2-14 and Fig 2-15 display results illustrating that when DG is implemented the service voltage is lowered because of the CVR method.

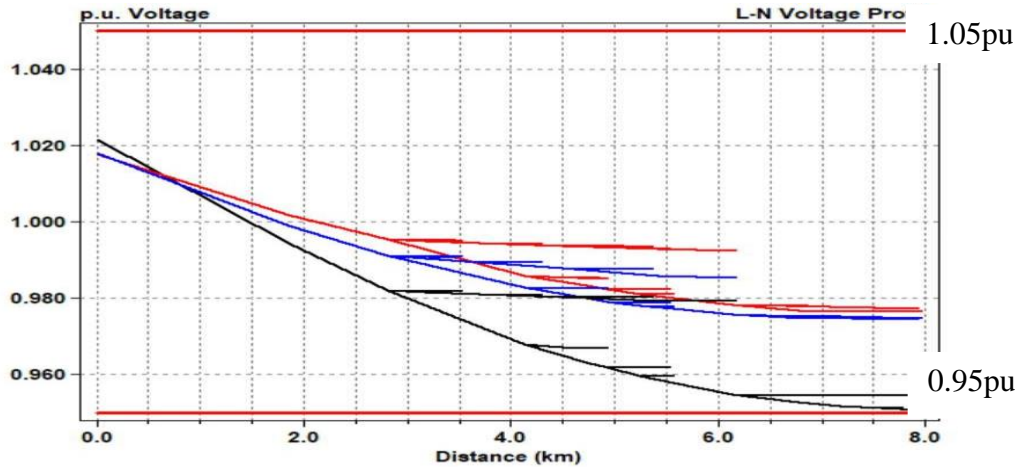


Fig. 2-14 Modified IEEE 37-bus system voltage profile for “No PV” penetration case

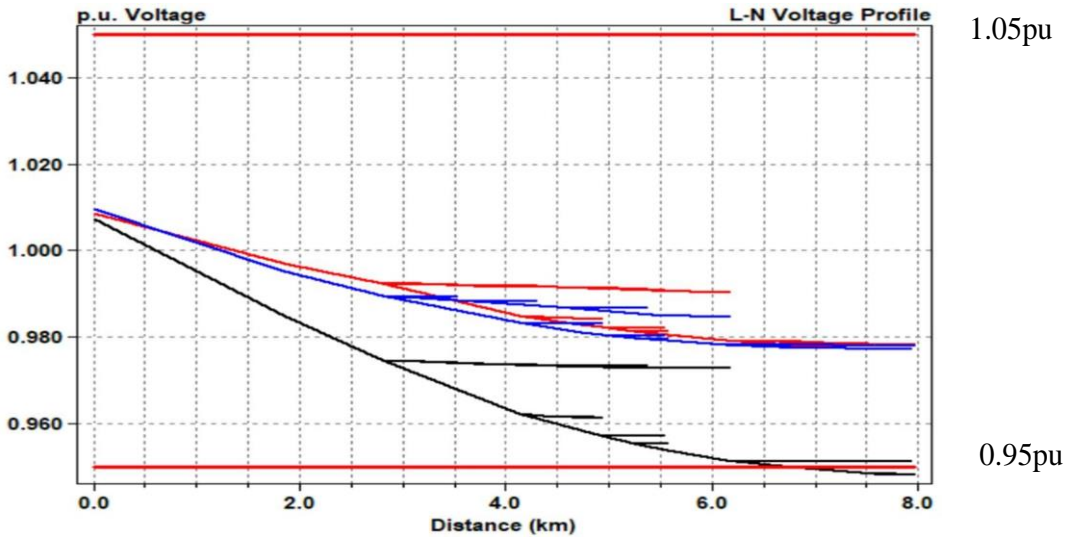


Fig. 2-15 Modified IEEE 37-bus system voltage profile for 20% PV penetration case

When DG is integrated into a distribution feeder voltage rise can also occur [8]. A CVR control algorithm is developed because of this occurrence lowering the service voltage along the distribution feeder while satisfying the ANSI C84.1 standard. Figs 2-16 and 2-17 present the 40% and 60% PV penetration cases voltage profiles respectively and due to the increase PV penetration, the voltage along the distribution feeder increases.

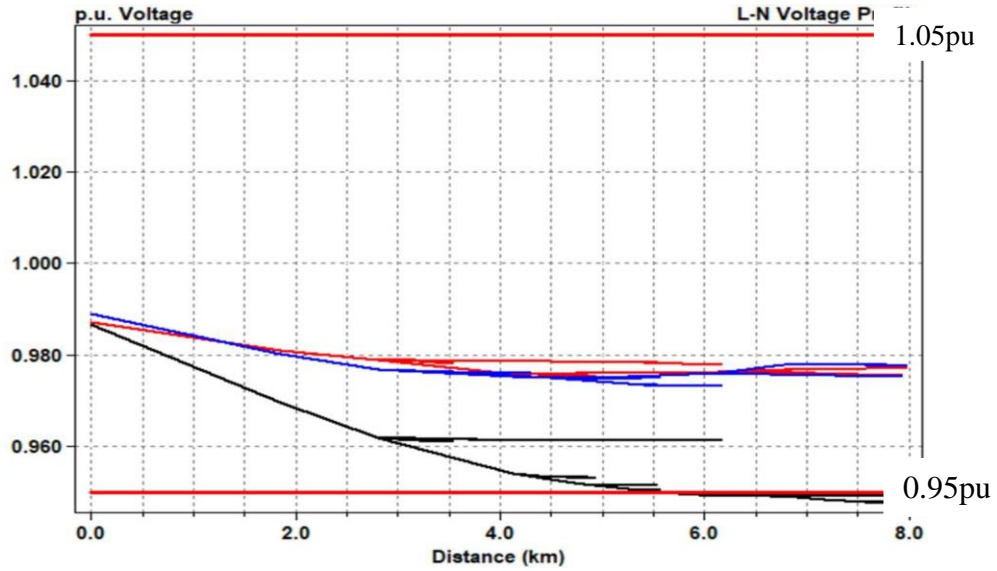


Fig. 2-16 Modified IEEE 37-bus voltage profile for 40% PV penetration case

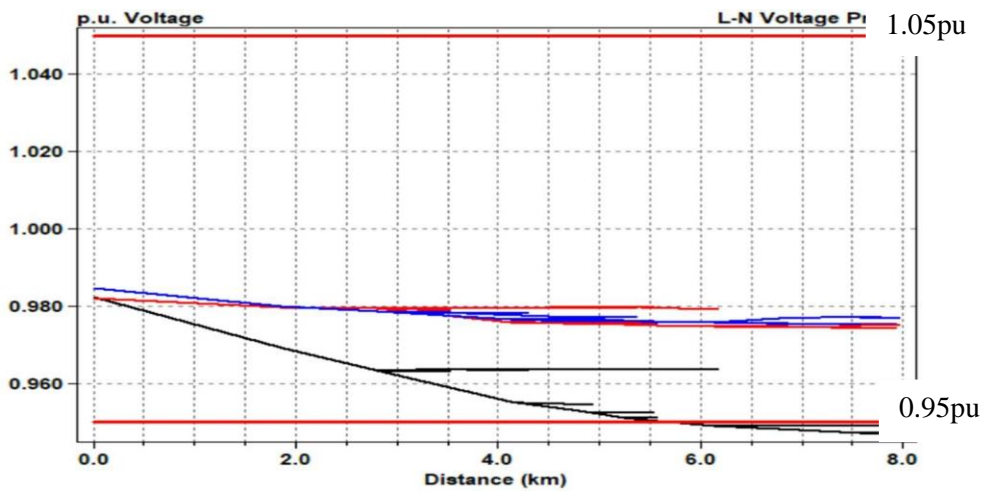


Fig. 2-17 Modified IEEE 37-bus voltage profile for 60% PV penetration case

DG can cause noticeable effects to a voltage profile of a distribution feeder. With the addition of DG, the direction of the power flow can be potentially reversed causing drastic fluctuations in the voltage on the consumer end [9]. These effects occurred in the 40% and 60% PV penetration cases which in turn the service voltages are reduced because of CVR/IVVC illustrated in Fig 2-16 and Fig 2-17.

2.8 Conclusions

This chapter was able to illustrate and explain the theoretical background of the selected case studies. CVR and IVVC when implemented simultaneously in a distribution system can reduce the amount of OLTC, VR and switched capacitor bank operations in a distribution system. However, CVR and IVVC alone is not able to reduce the number of operations under PV penetration scenarios [4]. The next chapter will discuss the implementation of smart PV inverter functions and their ability to provide reactive power and voltage control in a distribution system.

2.9 References

1. Matthew J. Reno, M.R (2017). Quasi-Static Time Series (QSTS) Simulations for Distribution System Analysis [Power point slides], Sandia National Laboratories <https://www.osti.gov/servlets/purl/1431692>
2. J. A. Azzolini, M. J. Reno and M. Lave, "Visualization Methods for Quasi-Static Time-Series (QSTS) Simulations with High PV Penetration," *2019 IEEE 46th Photovoltaic Specialists Conference (PVSC)*, 2019, pp. 0892-0899, doi: 10.1109/PVSC40753.2019.8980550.
3. Dr. Zhaoyu Wang, Z.W, Fankun Bu , F.B (2019). OpenDSS Tutorial and Cases [Power point slides] Department of Electrical and Computer Engineering, Iowa State University.
4. D. Symonette and J. C. Balda, "Evaluation of Single-Phase PV Smart Inverter Functions in Unbalanced Residential Distribution Systems," *2021 IEEE 12th International Symposium on Power Electronics for Distributed Generation Systems (PEDG)*, 2021, pp. 1-6, doi:10.1109/PEDG51384.2021.9494207.
5. Gonen, T. (2014). *Electric Power Distribution Engineering* (3rd ed.). CRC Press. <https://doi.org/10.1201/b16455>
6. H. Safar, "Power transmission line analysis using exact, nominal π , and modified π models," *2010 The 2nd International Conference on Computer and Automation Engineering (ICCAE)*, 2010, pp. 128-134, doi: 10.1109/ICCAE.2010.5451500.

7. R. C. Dugan, The Open Distribution System Simulator (OpenDSS), Electric Power Research Institute, Palo Alto, CA, USA, 2019. [20] A. Hariri, M. O. Faruque, R. Soman and R. Meeker, "Impacts and interactions of voltage regulators on distribution networks with high PV penetration," 2015 North American Power Symposium (NAPS), Charlotte, NC, USA, 2015, pp. 1-6, doi: 10.1109/NAPS.2015.7335212.
8. Bokhari *et al.*, "Experimental Determination of the ZIP Coefficients for Modern Residential, Commercial, and Industrial Loads," in *IEEE Transactions on Power Delivery*, vol. 29, no. 3, pp. 1372-1381, June 2014, doi: 10.1109/TPWRD.2013.2285096.
9. R. Singh, F. Tuffner, J. Fuller and K. Schneider, "Effects of distributed energy resources on conservation voltage reduction (CVR)," *2011 IEEE Power and Energy Society General Meeting*, 2011, pp. 1-7, doi: 10.1109/PES.2011.6039702.
10. V. Borozan, M. E. Baran and D. Novosel, "Integrated volt/VAr control in distribution systems," *2001 IEEE Power Engineering Society Winter Meeting. Conference Proceedings (Cat. No.01CH37194)*, 2001, pp. 1485-1490 vol.3, doi: 10.1109/PESW.2001.917328.

CHAPTER 3

SIMULATION PROCESS AND RESULTS

3.1 Introduction

The objective of this chapter is to analyze the simulation process and results for the modified IEEE 37-bus system and the utility feeder under different levels of PV generation. Before discussing the simulation process and results, smart PV inverter functionalities and characteristics must be understood. A smart inverter converts DC current into AC current to be injected into a power grid while simultaneously using smart functions to assist in reactive power control and voltage regulation [1]. For the simulation process, EPRI OpenDSS™ interfaced with MATLAB proved to be useful because of OpenDSS™ ability to support grid integration of Distributed Energy Resources (DER) using QSTS. Each smart function is studied under 20, 40 and 60% PV penetrations, respectively, with CVR/IVVC applied both selected distribution systems. The control scripts for the smart inverter functionalities such as the Volt/VAr (VV), Fixed Power Factor (FPF) and Dynamic Reactive Current (DRC) functions are modeled in OpenDSS™ in a separate ‘InvControl’ library that is contained in a set of control elements (CE’s) [2].

3.2 Implementation of Smart PV Inverter Functions in OpenDSS™

EPRI OpenDSS™ contains the smart PV inverter models that are comprised of two components such as the physical inverter components with regards to its KVA, KVA_r, irradiance and power factor (PF) sign (to determine whether it is injecting or absorbing reactive power) along with several other parameters [3]. The model for every PV inverter implemented is model in a ‘PV system’ that allows OpenDSS™ to identify the element as a power conversion element and DER. Fig. 3-1 shows the solar irradiance for PV systems which determines the power injected into the

grid via the PV inverters. Fig. 3-1 shows the PV generation over a 14-day period where specific control algorithms while integrated with the PV inverters modeled in OpenDSS™ are considered.

The factors that contributed to the design of the PV inverters in OpenDSS™ consisted of:

- Bus location
- Irradiance
- Apparent power rating
- Generation curve
- Cutout and cutin percentage

OpenDSS™ represents distributed generation (DG) in this case PV inverters as power conversion elements [3]. The ratings can be defined using the kW with the device's PF or its kVA with its PF. For the Smart inverters in both distribution systems, the apparent power with the PF is used to determine the desired amount of active and reactive powers injected into the point of common coupling (PCC) based on the solar irradiance curve. In other words, the curve in Fig. 3-1 represents the multiplier values which determines the amount of apparent power injected into the grid at specific period over 336 hours (14 days).

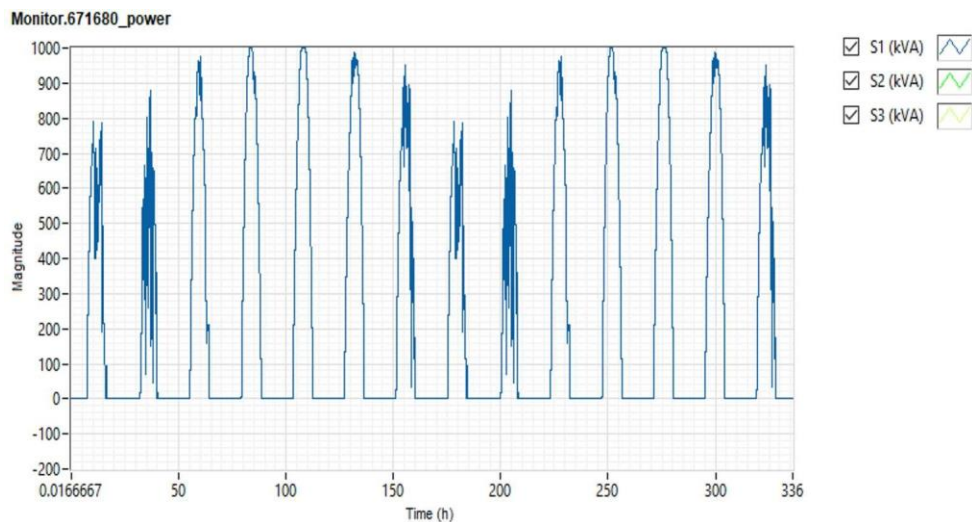


Fig. 3-1 Solar irradiance over a 14-day period

For the Smart inverters in both distribution systems, the apparent power with the PF is used to determine the desired amount of active and reactive powers injected into the point of common coupling (PCC) based on the solar irradiance curve. In other words, the curve in Fig. 3-1 represents the multiplier values which determines the amount of apparent power injected into the grid at specific period over 336 hours (14 days). The PF determines how much of that power will be active or reactive power and based on the sign of the PF value with a positive value meaning the inverter will be injecting leading reactive power and negative meaning the PF is lagging injecting a lagging reactive power at the PCC. Fig. 3-2 shows the fixed power factor script that was implemented in the smart PV inverters over 14 days. Fig. 3-2 contains the bus location of this specific inverter with a leading PF of 0.95 injecting a leading reactive power at the PCC. Fig. 3-3 is the Volt/VAr script that was created to simulate the Volt/VAr function for the PV inverters in the modified IEEE 37-bus system and utility feeder. The X and Y arrays determines the amount of leading or lagging reactive power injected into the grid at the PCC with respect to the per unit (pu) voltage. The Y arrays represents the reactive power, and the X array represents the pu voltage at which the desired level of reactive power is being injected. The reactive power value for the Volt/VAr function is determined using the linear equation $Y = mx + c$ in which $c=0$. M being the slope $m = \frac{Q}{0.05}$ and x representing the change in voltage at the PCC (V_{pcc}) such that $x = (1 - V_{pcc})$ to ensure the reactive power is injected at the PCC at the appropriate level to maintain the voltage within the ANSI C84.1 standard. Fig. 3-4 is the DRC script implemented in the PV inverters for the modified IEEE 37-bus system and utility feeder. The DRC function script operates like the Volt/VAr script however it determines whether a leading or lagging reactive current is injected at the PCC based on the ArGHiV and ArGLow which represent the rate of change for the pu voltage with respect to the reactive current.

```
New PVSystem.PV1 phases=1 bus1=701.1 kV=7.967
kVA=182 irrad=1 %cutin=0.05 %cutout=0.05
Pmpp=182 Daily=Mylrrad PF=0.95
```

Fig. 3-2 Phase A for PV system at bus 701 with a 0.95 leading power factor [4]

```
New XYCurve.vv_curve npts=4 XArray=
(0.5,0.95,1.05,1.5) Yarray=(1,1,-1.0,-1.0)
New InvControl.InvPVCtrl mode=VOLTVAR
voltage_curvex_ref=rated vvc_curve1=vv_curve
Event log = yes
```

Fig. 3-3 Open-DSS Volt/VAr function [4]

```
New InvControl.InvTestPVCtrl
mode=DYNAMICREACCURR DbVMin=0.95
DbVMax=0.985 ~ ArGraLowV=10.0
ArGraHiV=10.0 DynReacavgwindowlen=120s
EventLog=yes
```

Fig. 3-4 Open-DSS Dynamic reactive current function [4]

3.2.1 Implementing the FPF function in OpenDSSTM

The first smart PV inverter function that was selected was the fixed power factor function with a set PF of 0.95 leading. Table 3-1 shows the FPF ability to lower the OLTC operations when coordinated with CVR/IVVC. For this research, the PV penetration levels of 20%, 40% and 60% were studied with Fig. 3-5 showing the 60% case. The use of CVR/IVVC alone does not have the capability to reduce OLTC, VR and SCB operations however, when implemented with smart PV functions, the number of operations for these devices can be reduced. Table 3-1 illustrates the FPF function applied with CVR/IVVC and its ability to reduce the number of operations for the substation OLTC. The table shows that the number OLTC operations increases as the PV

Table 3-1 Effects of CVR/IVVC with Fixed Power Factor function (0.95 leading)

Case Study	Substation Power (MVA) All three feeders, no CVR, LTC = 122 V	PV Generation on main feeder at peak load	No CVR, LTC Operations	Substation Power (MVA) All three feeders, CVR	PV Generation on main feeder at peak load	CVR, LTC Operations
No PV	12.28 + j3.43 PF = 0.963 Lag Main feeder = 6.49 + j2.08 MVA	0 MVA	76	12.24 + j3.38 MVA PF=0.965 Lag Main feeder = 6.33 + j1.75 MVA	0 MVA	43
20% PV	9.31 + j 3.31 PF = 0.942 Lag Main feeder = 4.31 + j1.93 MVA	2.18 + j0.22 MVA	87	9.20 + j3.16 MVA PF = 0.946 Lag Main feeder = 4.27 + j1.37 MVA	2.04 + j0.12 MVA	12
40% PV	7.68 + j 2.99 PF = 0.932 Lag Main feeder = 2.01 + j1.75 MVA	4.48 + j0.35 MVA	130	7.48 + j2.8 MVA PF = 0.934 Lag Main feeder = 1.91 + j1.23 MVA	4.42 + j0.52 MVA	17
60% PV	5.29 + j 2.82 PF = 0.882 Lag Main feeder = 1.52 + j0.78 MVA	4.98 + j1.4 MVA	140	5.19 + j2.62 MVA PF = 0.893 Lag Main feeder = 1.59 + j0.35 MVA	4.74 + j1.3 MVA	19

penetration level increases along the distribution feeder. At 20% PV penetration, the OLTC operations increase by 13% in contrast to the no PV case. From 20% to 40% the number of operations increase at a higher percentage of 33% and the 40% to 60% case a 9% increase occurs which is the smallest difference in comparison to the no PV to 20% and 20% to 40% cases. Table 3-1 further illustrates CVR/IVVC implemented with the FPF function in the comparison to the no CVR cases. For the no PV case the number of operations for the OLTC decreases by 43% with just with CVR/IVVC being applied to the distribution feeder. However, at the 20% case the FPF function is being applied with CVR/IVVC and the OLTC operations decreases by 86%. The percentage for the decrease in operations in the 40% and 60% penetration levels are 86% and 87% respectively illustrating CVR/IVVC implemented with smart PV inverter functions, correlates with the reduction in OLTC and VR operations in high PV penetration scenarios [4].

Fig. 3-5 illustrates the PV inverter behavior over a 14-day period with the FPF function implemented. The PV inverters to inject a leading reactive power with a set power factor into the selected case studies lowering the lagging reactive power.

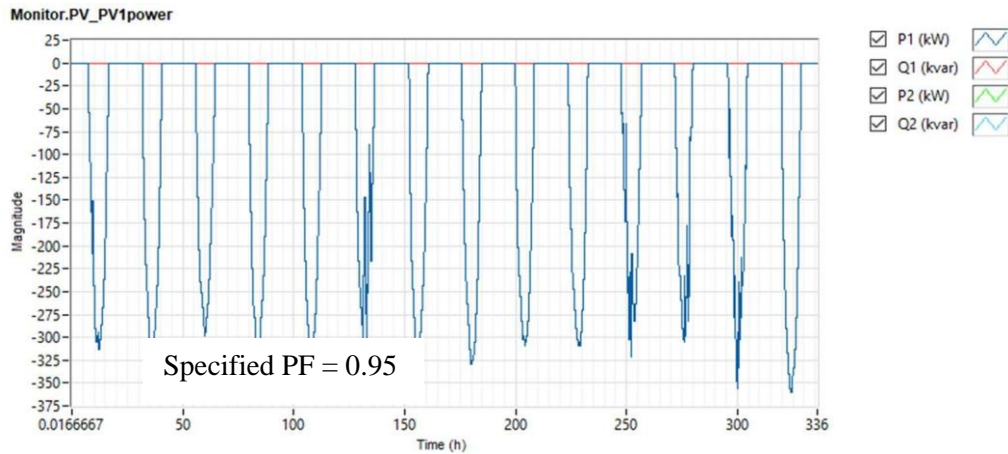


Fig. 3-5 PV system performing the FPF function for 60% PV penetration

This reduction in lagging reactive power leads to an improvement of the substation's power factor and an improvement in the voltage levels along the distribution feeder resulting in the OLTC to performing less operations over the considered 14-day period.

3.2.2 Implementing the Volt/VAr function in OpenDSSTM

The Volt/VAr function was also integrated into the smart PV inverters to provide voltage and reactive power support. Fig. 3-6 shows the Volt/VAr function curve as implemented on a PV inverter based on a XY curve implemented into OpenDSSTM. The Volt/VAr function provides a mechanism where DG can manage the VAR output in response to the PCC voltage of the distribution feeder [6]. The reactive power outputted by the PV inverter can change from leading to lagging or vice versa based off the distribution feeder's voltage level. This is further explained in Fig. 3-6 where the maximum service voltage is at 1.03 pu, a lagging reactive power is injected into the distribution feeder from the PV inverters to maintain the voltage profile in the ANSI C84.1 limit. While at 0.95 pu a leading reactive power is injected into the distribution feeder to ensure the voltage does not drop below the 0.95 pu limit. This ability allows the Volt/VAr function to not only maintain the service voltage within the $1.03 < \text{pu} < 0.95$ voltage limit but also allows the

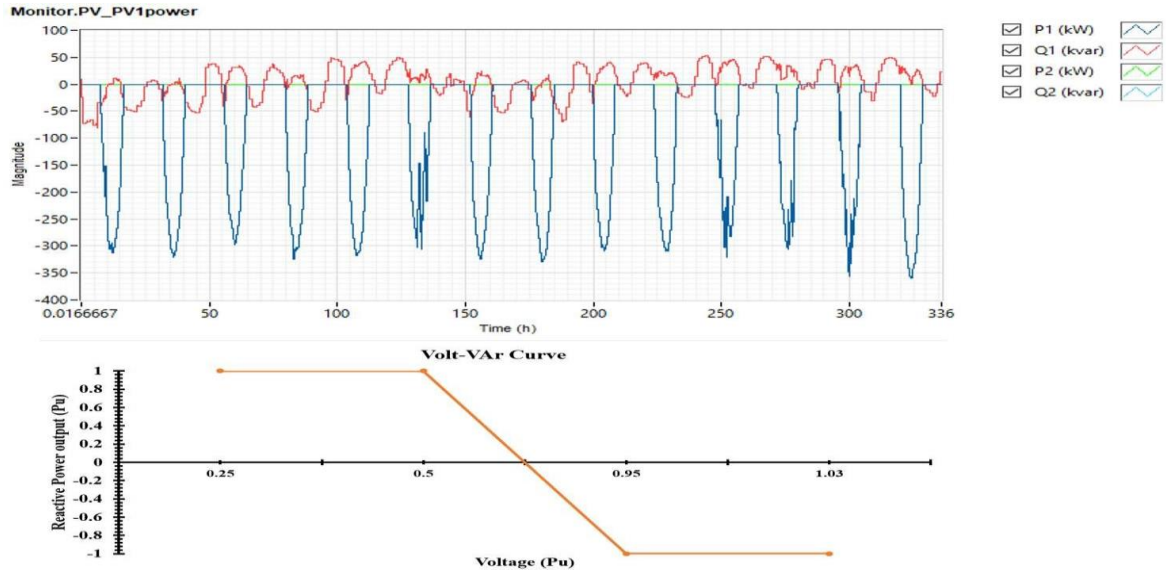


Fig. 3-6 PV system performing the VV function for 60% PV penetration

OLTC and SCBs to perform less tap changes and switching states with regards to voltage and reactive power control.

3.2.3 Implementing the DRC function in OpenDSSTM

The DRC function was integrated with CVR/IVVC and implemented into the smart PV inverters. The DRC function absorbs or injects reactive current as shown in Fig. 3-7 based on the premise of distribution feeder's current levels in relation to the voltage.

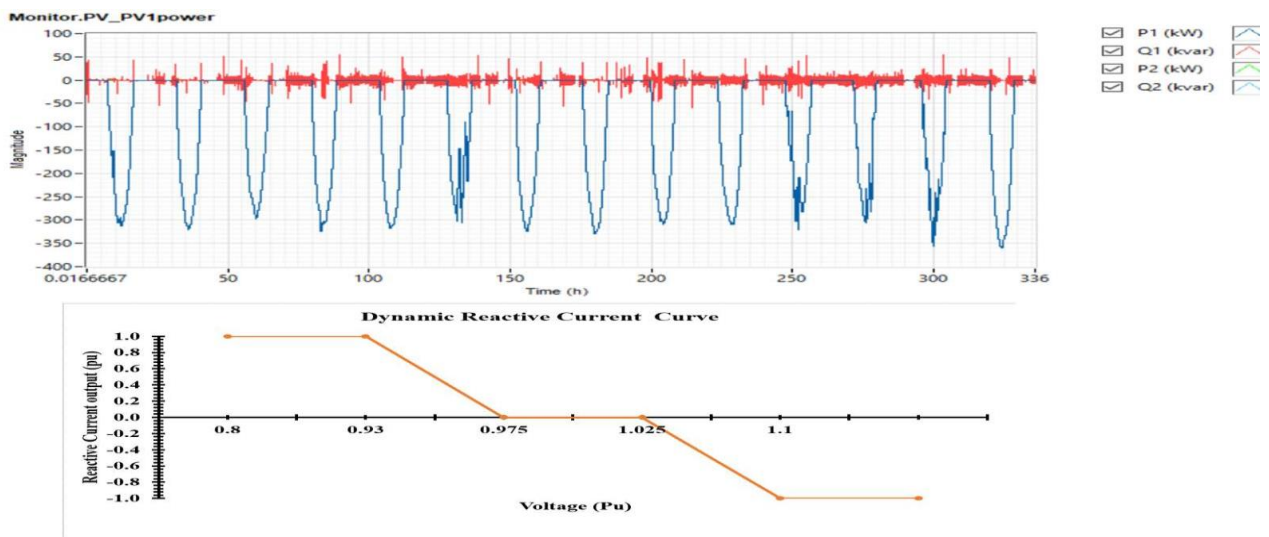


Fig. 3-7 PV system performing DRC function for 60% PV penetration

Under the DRC function the PV inverter absorbs or injects reactive current at the PCC like the Volt/VAr function; however, there are some dissimilarities. Fig 3-7 shows that at 0.93 pu, the PV inverter injects a leading reactive current into the grid while at 1.1 pu and lagging reactive current is injected into the grid. This in turn allows the OLTC and SCBs to perform less operations.

3.3 Simulation Results under Different PV Penetration Levels

A series of simulations were performed to verify the results and theoretical assumptions. Table 3-2 shows that the smart inverter functions can assist the OLTC and VR by reducing the number of operations and tap changes for the modified IEEE 37- bus system and the Utility feeder. From Table 3-2, the base case which represents no PV with a 2-volt bandwidth contains more operations than every other case. Reference [7] shows that as voltage changes and fluctuates, voltage profiles for distribution systems can experience unwanted voltage rises.

Table 3-2 Effects of smart PV inverter functions on OLTC for different PV penetration scenarios for the modified IEEE 37-bus system and Utility feeder

	No. of operation @ No PV penetration with Bandwidth = 2 V		No. of operation @ 20% PV penetration with Bandwidth = 2 V		No. of operation @ 40% PV penetration with Bandwidth = 2 V		No. of operation @ 60% PV penetration with Bandwidth = 2 V	
	37-Bus	U. F1	37-Bus	U. F1	37-Bus	U. F1	37-Bus	U. F1
	43	42						
Fixed Power Factor function	-	-	12	16	17	18	19	24
Volt/VAr Function	-	-	9	12	3	5	1	1
Dynamic Reactive Current function	-	-	43	40	50	46	56	52

However, from both case studies and analysis of the voltage profiles with the smart PV inverter functions implemented, the results shows that the PV inverters can assist in providing voltage and reactive power support. Table 3-3 shows the results for the SCB in the modified IEEE 37-bus system for 20%, 40% and 60% PV penetration.

The Volt/VAr function for all three cases contains the least number of operations while the DRC function possess the most operations for all three functions. The results displayed also shows similar results for both systems proving the Volt/VAr function to be the most effective. The Utility feeder is not represented in this table 3-3 because it only contains fixed capacitor banks which remain on regardless of KVAR conditions in the distribution feeder. The modified IEEE 37-bus system 3 SCBs were analyzed for each penetration percentage under each smart function and from observation of table 3-3 the Volt/VAr function proves to be the most effective function.

Table 3-3 Effects of smart PV inverter functions on SCBs for different PV penetration scenarios on the modified IEEE 37-bus system.

KVAr Rating	No PV Penetration For 300 KVAr SCB	No. of operations @ 20% PV penetration For 300 KVAr SCB	No. of operations @ 40% PV penetration For 300 KVAr SCB	No. of operations @ 60% PV penetration For 300 KVAr SCB
	86			
Fixed Power Factor function	-	24	36	58
Volt VAr function	-	10	16	56
Dynamic Reactive Current function	-	24	48	72

3.3.1 Volt/VAr function results with CVR/IVVC

The OLTC for the modified IEEE 37-bus system and the utility feeder with a downstream voltage regulator behavior are analyzed with the Volt/VAr function. Fig. 3-8 shows the number of tap changes for the modified IEEE 37-bus system OLTC for the 60% case with a 45 second delay with a 2-V bandwidth. The number of changes for the 60% PV penetration level shows 1 tap change. Fig. 3-9 illustrates the Volt/VAr function at 60% PV penetration for the utility feeder. Where the VR presents similar results verifying those of the modified IEEE 37- bus system; the utility feeder's VR also performs 1 tap change over 14 days (336 hours).



Fig. 3-8 OLTC operations for the VV function at 60% PV Penetration for the modified IEEE 37-bus system



Fig. 3-9 OLTC operations for the VV function at 60% PV Penetration for Utility feeder

3.3.2 DRC function results with CVR/IVVC

Fig. 3-10 shows the effects of the DRC function on the OLTC for the modified IEEE 37-bus system. The DRC function displays the greatest number of operations for all three functions with 56 operations, proving this function to be the least affective. Fig. 3-11 indicates the DRC function for the VR of the utility feeder which is compared to the other 2 functions implemented on the distribution feeder. For the DRC function 60% PV penetration case, number of operations were similar in value for the two distribution systems.

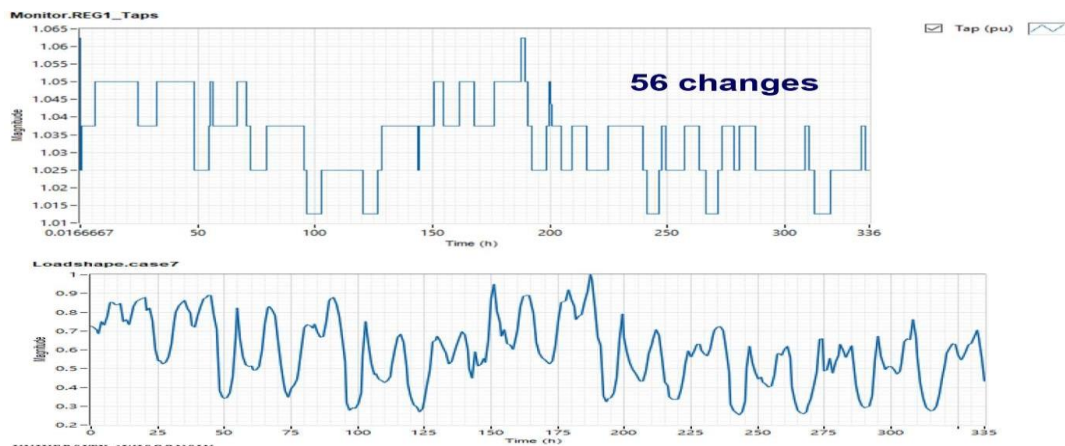


Fig. 3-10 OLTC operations for the DRC function at 60% PV penetration for the modified IEEE 37-bus system

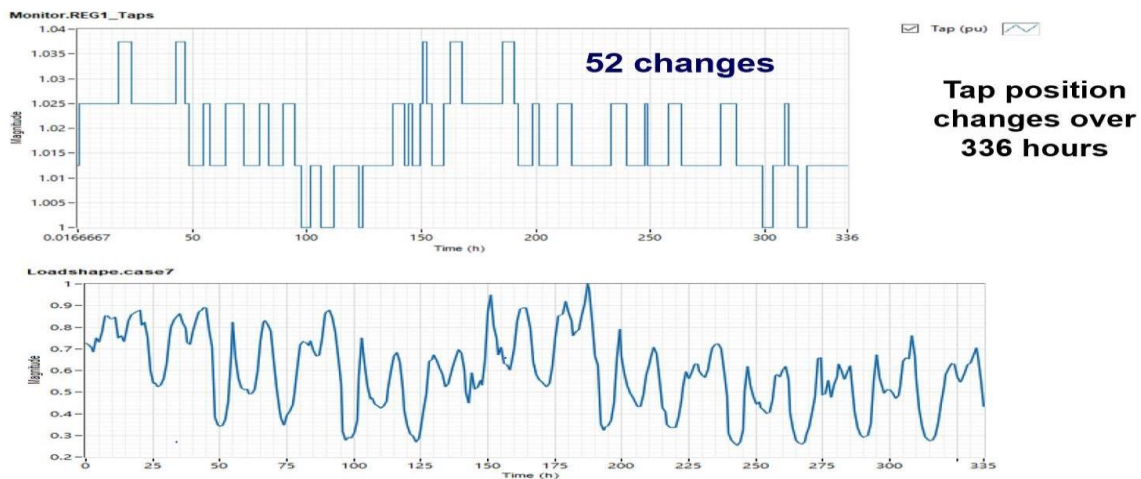


Fig. 3-11 OLTC operations for the DRC function at 60% PV penetration for Utility feeder

3.3.3 FPF function results with CVR/IVVC

Fig. 3-12 displays the number of tap changes for the substation OLTC implementing the FPF function at 60% PV penetration for the modified IEEE 37-bus system over a 14-day period. Fig. 3-13 indicates the number of tap changes for the VR in the utility feeder also over a 14-day period. The modified IEEE 37-bus system OLTC performed 19 taps changes in comparison to the utility feeder VR which performed 24 operations. The FPF function contained more operations than the Volt/VAr function but performed less operations in comparison to the DRC function.

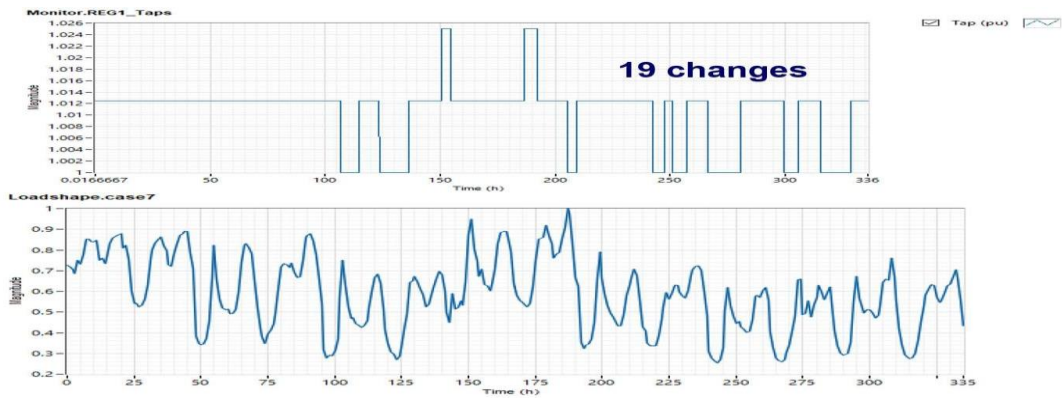


Fig. 3-12 OLTC operations for the FPF function at 60% PV penetration for modified IEEE 37-bus system



Fig. 3-13 OLTC operations for the FPF function at 60% PV penetration for Utility feeder

3.4 Conclusions

This chapter evaluated the impact of rooftop single-phase PV systems in unbalanced distribution systems with regards to the number switched capacitor bank operations and voltage regulator tap changes. Specific PV penetration scenarios were selected and with the use of CVR/IVVC the fixed power factor, Volt/VAr and Dynamic Reactive Current functions, the number of operations for the switched capacitor banks and voltage regulator operations were reduced. In summary, single-phase PV smart inverters providing VAr support proved to be effective in reducing the numbers of operations [5]. Chapter 3 shows that with the best-case function and with CVR/IVVC implemented, the number of operations for switched capacitor banks and voltage regulators can be reduced.

3.5 References

1. *Solar integration: Inverters and grid services basics.* (2012). Energy.gov. <https://www.energy.gov/eere/solar/solar-integration-inverters-and-grid-services-basics>
2. P. Radatz, C. H. S. Rocha, J. Peppanen and M. Rylander, "Advances in OpenDSS smart inverter modelling for quasi-static time-series simulations," *CIREC 2020 Berlin Workshop (CIREC 2020)*, 2020, pp. 243-246, doi: 10.1049/oap-cired.2021.0319.
3. R. C. Dugan, *The Open Distribution System Simulator (OpenDSS)*, Electric Power Research Institute, Palo Alto, CA, USA, 2019. [20] A. Hariri, M. O. Faruque, R. Soman and R. Meeker, "Impacts and interactions of voltage regulators on distribution networks with high PV penetration," 2015 North American Power Symposium (NAPS), Charlotte, NC, USA, 2015, pp. 1-6, doi: 10.1109/NAPS.2015.7335212
4. D. Symonette and J. C. Balda, "Evaluation of Single-Phase PV Smart Inverter Functions in Unbalanced Residential Distribution Systems," *2021 IEEE 12th International Symposium on Power Electronics for Distributed Generation Systems (PEDG)*, 2021, pp. 1-6, doi:10.1109/PEDG51384.2021.9494207.

5. Modeling High-Penetration PV for Distribution Interconnection Studies: Smart Inverter Function Modeling in OpenDSS, Rev. 2, EPRI, Palo Alto, CA: 2013. 3002002271.
6. A. Mohapatra, S. Behera, S. Nayak and B. K. Panigrahi, "A study on DG and capacitor placement in radial distribution system," 2012 IEEE International Conference on Power Electronics, Drives and Energy Systems (PEDES), Bengaluru, 2012, pp. 1-6, doi: 10.1109/PEDES.2012.6484268.
7. R. Singh, F. Tuffner, J. Fuller and K. Schneider, "Effects of distributed energy resources on conservation voltage reduction (CVR)," 2011 IEEE Power and Energy Society General Meeting, Detroit, MI, USA, 2011, pp. 1-7, doi: 10.1109/PES.2011.6039702.

CHAPTER 4

UTILITY FEEDER 1 AND UTILITY FEEDER 2 CASE STUDIES IN TYPHOON HIL

4.1 Introduction

In previous chapters OpenDSSTM - based QSTS power flows were conducted on the selected case studies. This chapter analyzes each case studies in real-time scenarios under CVR/IVVC implementation. From a control aspect, Conservation Voltage Reduction (CVR) is a simplified demand minimization because the direction of the change in voltage is predefined [1]. CVR is typically implemented during peak load hours in a distribution system where it is most needed to reduce power losses during high demand. In the selected case studies, peak load scenarios are implemented with CVR to show the effects of the method. Integrated Volt-VAr Control (IVVC) is simultaneously applied with CVR to further reduce power losses and assist in voltage regulation. By integrating Switch Capacitor Bank (SCB) and Voltage Regulator (VR) control methods, IVVC can improve the voltage profile while minimizing losses [2]. The objective of this chapter is to explain the process for implementing CVR and IVVC in Typhoon HIL, a hardware- in the loop tool capable of real time simulation studies.

4.2 Typhoon HIL Summarized Description

Typhoon HIL is a current generation real time processing platform that is used to verify stability, fault scenarios and power flow analysis. The real time capability allows connection to hardware for evaluation without the need of having the entire system, a distribution feeder in the case of this thesis topic. Each selected case study is modeled in the Typhoon HIL schematic editor and panel initialization and simulated in the pre-built SCADA panel displayed in Fig. 4-1.


```

Panel Initialization - (c102 feeder.cus)
68 solver_ = ["lbfgs", "sgd", "adam"]
69 user_classifier = MLPClassifier(activation=activation_[3], solver=solver_[2],
70 ..... learning_rate_init=0.007, random_state=1,
71 ..... hidden_layer_sizes=(30, 50, 11, 9, 3), max_iter=500,
72 ..... early_stopping=False, n_iter_no_change=50, shuffle=True)
73
74 Vn = 23900.3
75 vphase_peak_to_pu = 1 / (np.sqrt(2 / 3.0) * Vn)
76 t_samp = hil.get_sim_step() # Simulation sampling time
77 freq_samp = 1/t_samp # Sampling frequency
78 decimation = 10
79 freq_grid = 60 # Grid frequency
80 N_grid_cycles = 4 # Total grid cycles to be captured
81 N_samp = int(freq_samp * N_grid_cycles / decimation / freq_grid) # Number of samples to be captured
82 if (N_samp % 2) != 0:
83     N_samp += 1
84
85 # store the widget id
86 #w_id = "b80ba01c888711eb96041c1bb5b93d00"
87 #wh = panel.get_widget_by_id(w_id)
88
89 def capture_signals(return_dict, switch_name = "", training_mode=True):
90     .....
91     .....
92     global user_classifier
93     global n_cap_train
94     .....
95     .....
96     capture_counter = return_dict.get("capture_counter")
97     .....
98     initial_state = panel.get_property_value(wh, prop_name="state")
99     panel.set_property_value(wh, prop_name="state", prop_value="Capture")
100
101 # signals to be captured
102 channel_settings = ["NODE.DG.Va", "NODE.DG.Vb", "NODE.DG.Vc",]

```

Fig. 4-1 Pre-built SCADA initialization panel in Typhoon HIL

The Pre-Built SCADA panel is built using Python programming language and is designed in schematic editor and compiled to initialize the start of the simulation. The Pre-Built SCADA panel python program is included in Appendix B. Once the system is compiled, it is simulated in the virtual HIL producing real-time feedback with a 120us execution rate. The virtual HIL is an offline simulator that brings the capabilities of a physical HIL device to the computer. To conduct simulations each case study is designed in the schematic editor using the power system design principles discussed in Chapter 2.

4.2.1 Modeling the infinite bus

For the selected case studies, the infinite bus models were modeled using the methods and principles shown in Chapter 2 and implemented in a three-phase voltage source shown in Fig. 4-2, which is available in the schematic editor component library. The model panel initialization is used to specify global variables and functions that are used in the design model using Python programming. The model initialization script will be further discussed because it is used to implement the loads, capacitor banks (CB) and voltage regulators (VRs) in the selected distribution systems and is displayed in appendix B.

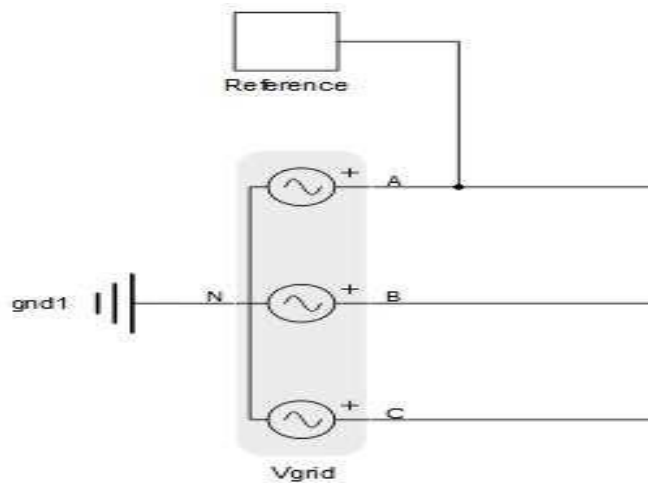


Fig. 4-2 Three-phase voltage source representing infinite the bus in Typhoon HIL

4.2.2 Modeling distribution feeders

Using the equations and models shown in section 2.3.2, the transmission line segment impedances were inputted into the model initialization panel. The transmission lines models were selected from the schematic power systems library. The declared variables in the model initialization panel are inputted into the transmission line segments in the schematic editor. Fig. 4-3 displays the graphic of transmission line segments used to model feeders.



Fig. 4-3 Transmission line segments graphic in Typhoon HIL

4.2.3 Load modeling

Applying section 2.3.3, the load for each case is modeled and attached to the distribution feeder. In Typhoon HIL, distribution loads are modeled in a single, two and three-phases as well a delta or wye connection and modeled as a constant impedance. For the single and two-phase loads each load, was modeled as a subsystem, which contained a parallel RL load illustrated in Fig. 4-4, and each R and L value was initialized in the model initialization script. For the three-phase loads shown in Fig. 4-5, the components are available in the schematic power systems library and parameters for each load are inputted into the selected load component. The loads in OpenDSS™ varied because of the dynamic load curve implemented over 14 days considering that a QSTS was performed. With the case of utility feeders 1 and 2 in Typhoon HIL, the loads were modeled as static loads during peak load time simulating a real-time scenario.

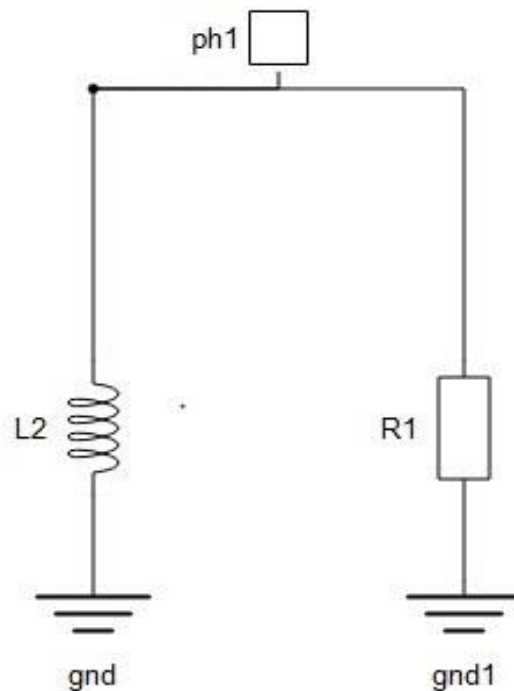


Fig. 4-4 Schematic of load model in Typhoon HIL

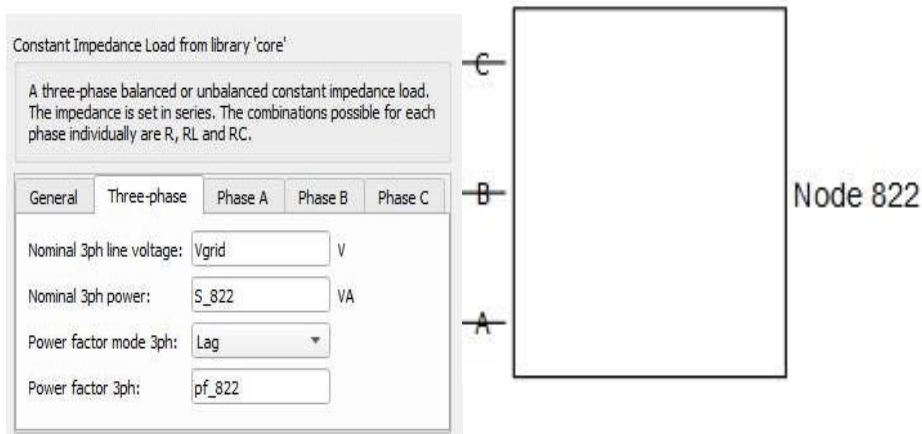


Fig. 4-5 Three phase load component and parameters

4.2.4 Power factor correction and capacitor bank placement

Power factor correction was carried for both utility feeders using the theoretical concepts of section 2.3.4 of Chapter 2. Utility feeders 1 and 2 contain only fixed capacitor banks (FCB) with utility feeder 1 contains 3 600 kVAr (FCBs) and utility feeder 2 3 FCB of 600, 1200 and 300 kVAr, respectively. The capacitor banks were modeled in Typhoon HIL’s schematic editor and initialized in the model initialization script. The capacitor banks were modeled as shown in Fig. 4-6 and connected in shunt along the transmission line based on location best suited for PFC by using concepts given in section 2.3.4.

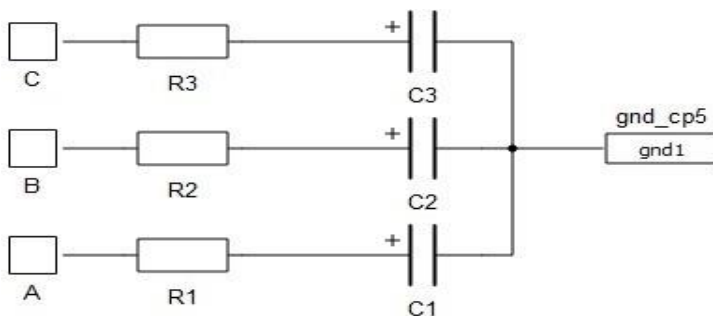


Fig. 4-6 Schematic of capacitor bank layout in Typhoon HIL

4.3 Selected Distribution Feeders

Utility feeders 1 and 2 were selected case studies that were modeled in Typhoon HIL. The behavior for both feeders are analyzed at peak load conditions with CVR/IVVC implemented. Utility feeder 1 is addressed in chapter 2 and is further analyze is studied in this chapter using typhoon HIL however, Utility feeder 2 is introduced in this chapter.

4.3.1 Utility feeder 1

Using section 2.4.2 as a reference, utility feeder 1 as shown in Fig. 4-7, is modeled in Typhoon HIL with CVR and IVVC coordinated together. By applying CVR/IVVC, as illustrated in Fig. 4-8 the voltage profile satisfies the lower half of the ANSI C84.1 standard with the substation bus voltage at 1 pu and bus 36 at 0.95pu at the of the feeder.

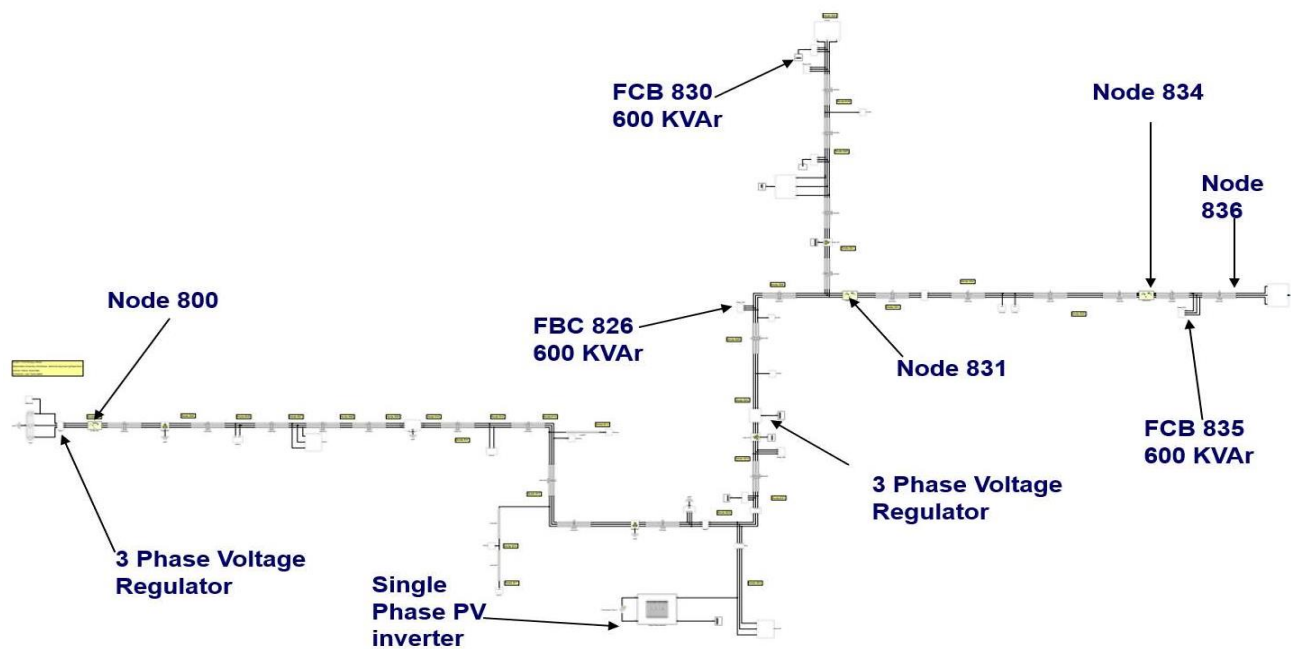


Fig. 4-7 Utility feeder 1 Typhoon HIL model

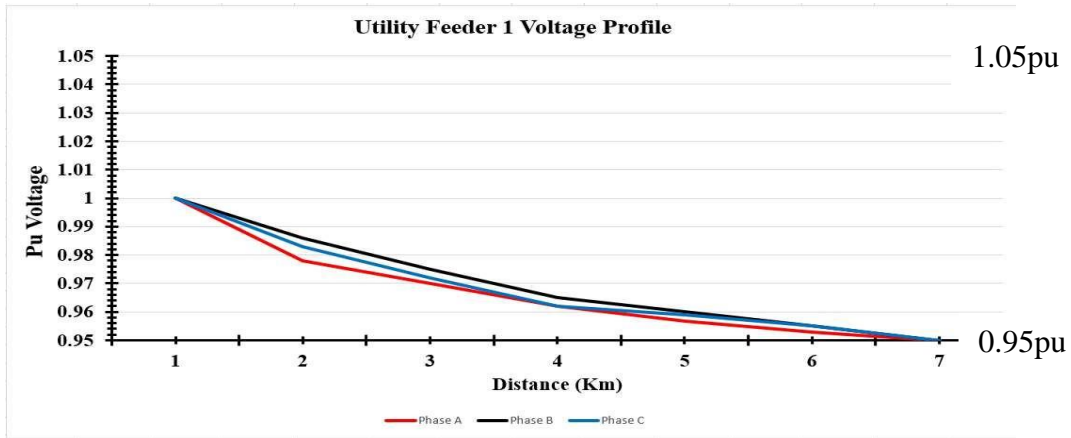


Fig. 4-8 Utility feeder 1 Voltage Profile

4.3.2 Utility feeder 2

Utility feeder 2 is the second feeder that is modeled in Typhoon HIL using the same design process for the modified IEEE 37-bus system and utility feeder 1. Fig. 4-9 displays the schematic for Utility feeder 2 modeled in Typhoon HIL. CVR/IVVC was applied to Utility feeder 2 satisfying the ANSI C84.1 requirements as shown in Fig. 4-10 with the substation bus voltage being 1 pu and bus 32 being 0.95 pu at the end of the feeder. Utility feeder 2 main parameters are given in Table. 4-1.

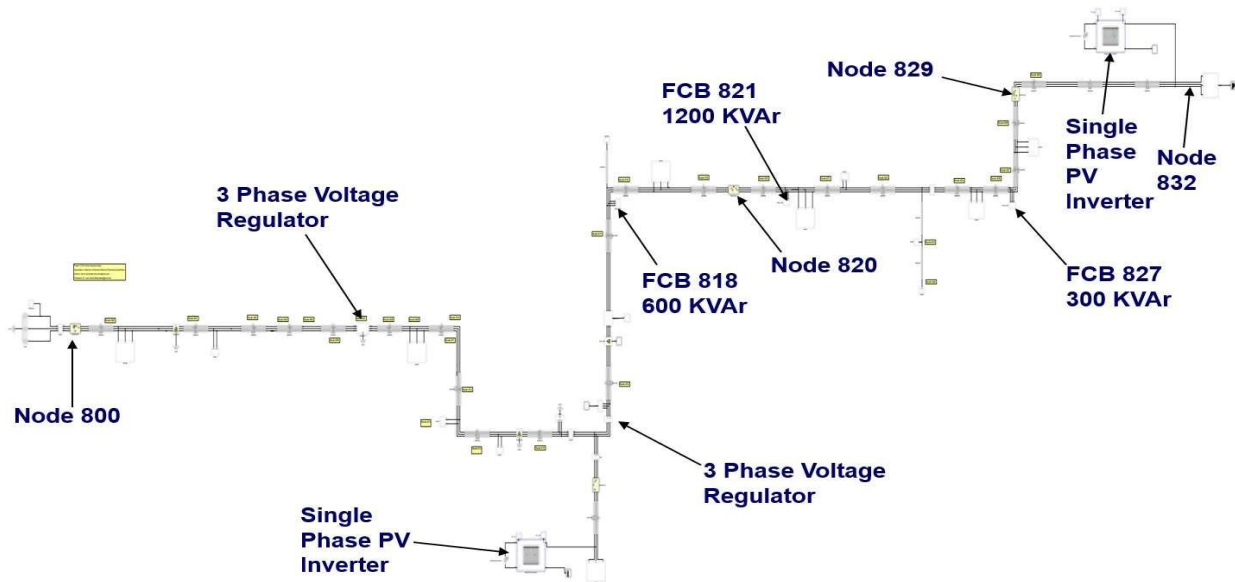


Fig. 4-9 Utility feeder 2 Typhoon HIL model

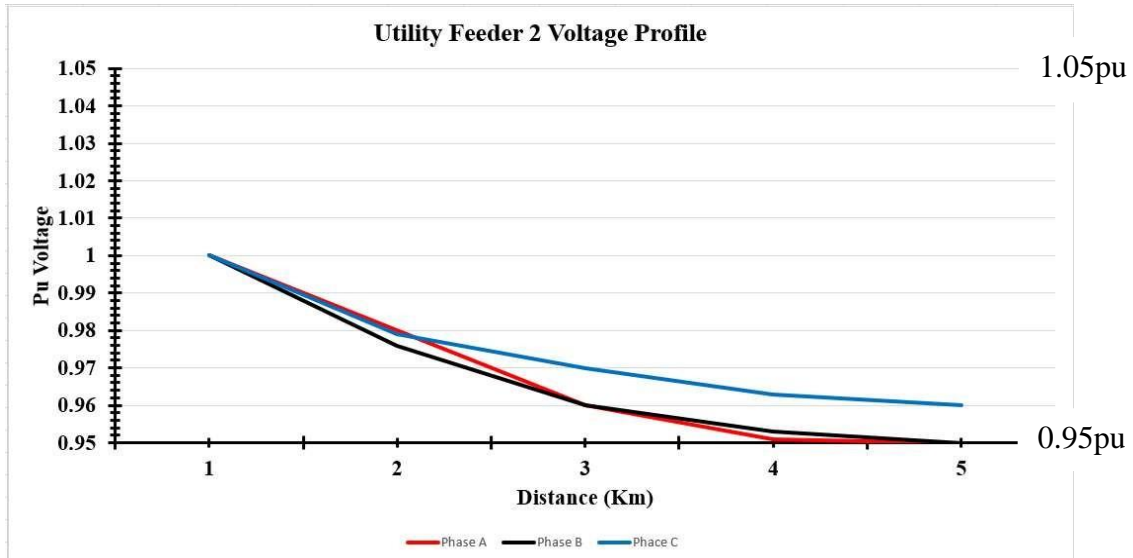


Fig 4-10 Utility feeder 2 Voltage Profile

Table. 4-1 Utility feeder 2 main characteristics

Sub transmission voltage (kV)	115
System voltage (kV)	13.8
kW Demand (kW)	4371
kVAr Demand	2698
Amp Demand (A)	198
PF Demand	0.91
Service xmfr connected (MVA)	20708
No. of voltage regulators	2
No. of fixed capacitors banks	3
No. of switch capacitor banks	0

4.4 Conclusions

This chapter illustrated the effects CVR and IVVC implemented simultaneously in a utility feeder through real time simulations enabled in Typhoon HIL. By reducing the service voltage of

a distribution feeder while ensuring that ANSI C84.1 standard is not violated, energy consumption can be reduced [3]. Furthermore, by implementing IVVC, VRs and OLTCs operations can be reduced to some extent due to flatter voltage profiles [4]. These two control methods were analyzed simultaneously at peak load in Typhoon HIL. Improvements in the voltage profile for both feeders were observed.

4.5 References

1. Roytelman and J. Medina, "Volt/VAR control and Conservation Voltage Reduction as a function of advanced DMS," *2016 IEEE Power & Energy Society Innovative Smart Grid Technologies Conference (ISGT)*, 2016, pp. 1-4, doi: 10.1109/ISGT.2016.7781180.
2. V. Borozan, M. E. Baran and D. Novosel, "Integrated volt/VAr control in distribution systems," *2001 IEEE Power Engineering Society Winter Meeting. Conference Proceedings (Cat. No.01CH37194)*, 2001, pp. 1485-1490 vol.3, doi: 10.1109/PESW.2001.917328.
3. R. Singh, F. Tuffner, J. Fuller and K. Schneider, "Effects of distributed energy resources on conservation voltage reduction (CVR)," *2011 IEEE Power and Energy Society General Meeting*, 2011, pp. 1-7, doi: 10.1109/PES.2011.6039702.
4. S. Rahimi, M. Marinelli and F. Silvestro, "Evaluation of requirements for Volt/Var control and optimization function in distribution management systems," *2012 IEEE International Energy Conference and Exhibition (ENERGYCON)*, 2012, pp. 331-336, doi: 10.1109/EnergyCon.2012.6347777.

CHAPTER 5

CONCLUSIONS AND FUTURE WORK

5.1 Conclusions

As elaborated in Chapter 1, Distribution Generation (DG) based on solar power when implemented in high photovoltaic (PV) penetration scenarios can increase the number of operations for VRs, OLTCs, and SCB's [1-3]. This effect is caused by erratic weather patterns causing instabilities and bringing about unwanted voltage fluctuations. The evaluation of single-phase smart PV inverters was conducted from a decentralized standpoint in a distribution system. The three functions analyzed were the Fixed Power Factor function (FPF), Volt/VAr (VV) function and the Dynamic Reactive Current (DRC) function. Each function was evaluated with Integrated Volt/VAr Control and Conservation Voltage Reduction (CVR/IVVC) applied from a decentralized control standpoint to analyze the effects of DG ability to provide reactive power and voltage support. With the use of CVR/IVVC and PV smart inverter functions, the number of operations for these devices can be lowered by an average of 72% with some functions being more effective than others. In summary, single-phase smart PV inverters proved to be effective in reducing the number of operations while providing VAr support from a decentralized control standpoint. Furthermore, single-phase PV smart inverters has the capabilities to improve the voltage profile of a distribution system without having to be owned by the electric utility [2]. However, selecting the proper function (e.g., Volt/VAr function) is important in obtaining the most effective results.

The principles and theory behind the analysis of DG and the selection of case studies was presented in Chapter 2 that also introduced the distribution software package EPRI OpenDSS™,

used to analyze the selected case studies using the QSTS algorithm. This was followed by the application of the smart PV inverter functions in the selected MATLAB/OpenDSS platform in chapter 3. The complete simulation process of the case studies was conducted at 20%, 40% and 60% PV penetration scenarios to study the behavior of the VRs, SCBs and OLTCs under these conditions. The implementation of CVR/IVVC in typhoon HIL on selected case studies at peak load was addressed in Chapter 4. The theoretical methodology applied in Chapter 2 was followed in Chapter 4 to model the case studies in Typhoon HIL where the use of CVR/IVVC was proven.

5.2 Recommendation for Future Work

The following subsections contains recommendations for future research based on the existing solutions and simulations of the designed case studies. Future work for this research will further address the role of smart PV inverters in Unbalanced Residential Distribution Systems with regards to QSTS studies with hardware implementation, restoration practices and microgrid applications.

5.2.1 *PHIL co-simulation Architecture*

(Power Hardware in the Loop) PHIL co-simulation architecture is the development of a dual software simulation method that integrates PHIL with a larger distribution system simulation using of a quasi-steady-state modeling tool commonly used by utilities for distribution simulations [4]. The FPF, VV and DRC functions will be further studied with the use of PHIL compatible with a QSTS. For the continuation of this work, a co-simulation method that enables integrated PHIL and a QSTS algorithm to be compatible must be developed. The performance of the selected

MATLAB/OpenDSS platform and Virtual HIL would not meet the requirements for a PHIL co-simulation due to a lack of PHIL hardware and a (Device under test) DUT.

5.2.2 Role of single-phase smart PV inverters in supporting URDS restoration practices

Fault Location Isolation and Service Restoration (FLISR) practices is a smart grid application that operates from an Advanced Distribution Management System (ADMS) platform that gives a power grid self-healing characteristic. Fig. 5-1 illustrates an FLISR scenario in which the single-phase smart PV inverters is providing power to the isolated area of the modified IEEE 37-bus system.

Distributed Energy Resources (DERs) have the possibility to provide FLISR applications to a utility distribution system and must be ensured that it functions in an integrated manner while operating reliably in the presence of DERs [5]. An area of research could be evaluating smart PV inverter functions from a centralized standpoint bringing about the use of centralized control and FLISR practices.

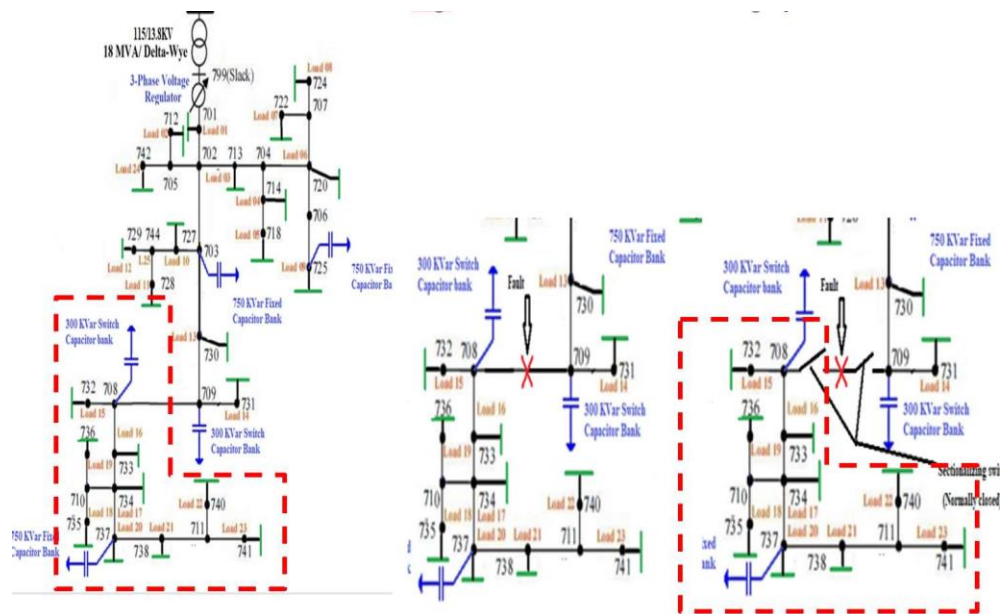


Fig. 5-1 FLISR scenario for modified IEEE 37-bus system

5.2.3 Evaluation of islanded operations for unbalance residential distribution systems

The proposed solution is an essential aspect to microgrids especially in single-phase scenarios. The operation in islanded mode in restoration practices can be implemented with conservation voltage reduction (CVR) and integrated Volt/VAr control (IVVC) while addressing the need for energy storage systems (ESSs). A distribution software package that does not need a conventional source to be attached to the system while able to perform a QSTS based simulation would be useful to continue this work.

5.3 References

1. A. Hariri, M. O. Faruque, R. Soman and R. Meeker, "Impacts and interactions of voltage regulators on distribution networks with high PV penetration," *2015 North American Power Symposium (NAPS)*, 2015, pp. 1-6, doi: 10.1109/NAPS.2015.7335212.
2. D. Symonette and J. C. Balda, "Evaluation of Single-Phase PV Smart Inverter Functions in Unbalanced Residential Distribution Systems," *2021 IEEE 12th International Symposium on Power Electronics for Distributed Generation Systems (PEDG)*, 2021, pp. 1-6, doi:
3. K. Alboaouh and S. Mohagheghi, "Impact of Rooftop Photovoltaics on the Distribution System," *Journal of Renewable Energy*, 2020. 1- 23. 10.1155/2020/4831434
4. B. Palmintier, B. Lundstrom, S. Chakraborty, T. Williams, K. Schneider and D. Chassin, "A Power Hardware-in-the-Loop Platform with Remote Distribution Circuit Cosimulation," in *IEEE Transactions on Industrial Electronics*, vol. 62, no. 4, pp. 2236-2245, April 2015, doi: 10.1109/TIE.2014.2367462.
5. A. Pratt, H. Padullaparti, Y. Ngo and H. Arant, "Defining a Use Case for the ADMS Test Bed: Fault Location, Isolation, and Service Restoration with Distributed Energy Resources," *2021 IEEE Power & Energy Society Innovative Smart Grid Technologies Conference (ISGT)*, 2021, pp. 1-5, doi: 10.1109/ISGT49243.2021.9372254.

APPENDIX A

OPENDSS AND MATLAB SCRIPTS

The MATLAB and OpenDSS™ scripts are written below for the selected case studies. This Appendix contains the MATLAB/OpenDSS™ COM interface, transmission line code segments, load scripts, capacitor bank scripts, conductor sizing Table A.5 and single-phase PV inverter models.

A.1 MATLAB main.m File

```
clear;

DSSObj = actxserver('OpenDSSEngine.DSS');

if ~DSSObj.Start(0)
disp('Unable to start the OpenDSS Engine');
return
end
DSSText = DSSObj.Text;
%[DSSCircObj, DSSText, gridpvPath] = DSSStartup;
DSSCircuit = DSSObj.ActiveCircuit;
DSSCircuit.methods;
DSSCircuit.get;
DSSCircuit.Lines.methods;
DSSCircuit.Lines.get;
DSSCircuit.Lines.LineCode;
DSSCircuit.Capacitors.get;
DSSCircuit.Capacitors.Name;
%DSSText.command= 'Compile""gridpvPath"(C:\Users\lamar\Downloads\Revised\10%
PV\MasterIEEE37.dss)';

DSSText.Command='Compile (C:\Users\lamar\Downloads\matlab and simulink\37 bus system
with daily mode\IEEE 37 bus system with daily mode\MasterIEEE37.dss)';% Path where Master
and its associated files are stored.
%%
DSSText.Command='batchedit load..* Model=8 status=variable Vminpu=0.95 ZIPV=(0.5, 0,
0.5, 1, 0, 0, 0.95)';
%%
DSSText.Command='export meter';
```

```

DSSText.Command='batchedit load.* daily=case7';
DSSSolution=DSSCircuit.Solution;
DSSText.Command='set maxcontroliter=100';

DSSText.Command='set mode=daily stepsize=1m number=1';
DSSText.Command = 'Set Controlmode=time';

% Set transformer element to beginning
DSSCircuit.Transformers.first;
% Get total number of transformers
numXfmr = DSSCircuit.Transformers.count;
% Preallocate
xfmrNames = cell(numXfmr, 1);
% Iterate
for ii = 1:numXfmr
    %Get current transformer name
    xfmrNames{ii} = DSSCircuit.Transformers.Name;
    % Advance to next transformer
    DSSCircuit.Transformers.Next;
end
% Note that there are currently no generators
DSSCircuit.Generators.get;
% Add PV in the form of a generator object
DSSText.command = 'new generator.PV bus1= 701 phases=3 kv=7.967 kw=500 pf=1
enabled=true';
% You can now see the generator that was added
DSSCircuit.Generators.get;
% Set it as the active element and view its bus information
DSSCircuit.SetActiveElement('generator.pv');
DSSCircuit.ActiveElement.BusNames
% Now change it to another bus and observe the change
DSSText.command = 'edit generator.PV bus1=n1325391 kv=13.2';
DSSCircuit.ActiveElement.BusNames
datapoints=20160;
for i=1:datapoints
    DSSSolution.Solve;
    DSSCircuit.Capacitors.Name=('C730');
    medium=DSSCircuit.Capacitors.States;
    CapState1(i)=medium(1);
    DSSCircuit.Capacitors.Name=('C711');
    medium1=DSSCircuit.Capacitors.States;
    CapState2(i)=medium1(1);
    DSSCircuit.RegControls.Name = ('creg1a');
    Regtap1(i) = DSSCircuit.RegControls.TapNumber;
    DSSCircuit.RegControls.Name = ('creg1b');
    Regtap2(i) = DSSCircuit.RegControls.TapNumber;
end

```

```

DSSCircuit.RegControls.Name = ('creg1c');
Regtap3(i) = DSSCircuit.RegControls.TapNumber;
DSSCircuit.RegControls.Name = ('creg2a');
end
nt1=datapoints/14;
for day=1:14
tap1_no(day)=0;
tap2_no(day)=0;
tap3_no(day)=0;
tap4_no(day)=0;
tap5_no(day)=0;
tap6_no(day)=0;
cap1_no(day)=0;
cap2_no(day)=0;

for j=1+((day-1)*nt1):((day-1)*nt1)+(nt1-1)
if Regtap1(j)~=Regtap1(j+1)
tap1_no(day)=tap1_no(day)+abs(Regtap1(j)-Regtap1(j+1));
end
if Regtap2(j)~=Regtap2(j+1)
tap2_no(day)=tap2_no(day)+abs(Regtap2(j)-Regtap2(j+1));
end
if Regtap3(j)~=Regtap3(j+1)
tap3_no(day)=tap3_no(day)+abs(Regtap3(j)-Regtap3(j+1));
end

if CapState1(j)~=CapState1(j+1)
cap1_no(day)=cap1_no(day)+abs(CapState1(j)-CapState1(j+1));
end
if CapState2(j)~=CapState2(j+1)
cap2_no(day)=cap2_no(day)+abs(CapState2(j)-CapState2(j+1));
end
end
end
tap1_no
tap2_no
tap3_no
cap1_no
cap2_no

DSSText.Command='set OpenDSSViewer=true';
DSSText.Command='plot monitors object=L1_power channels=(1 3 5)';
DSSText.Command='plot monitor object=711741_voltage channels=(1 3 5)';
DSSText.Command='plot monitor object=Reg1_voltage channels=(1 3 5)';
DSSText.Command='plot monitor object=Reg2_voltage channels=(1 3 5)';

```

```

DSSText.Command='Export monitors SubXF_voltage';
DSSText.command='plot monitors object=PV_PV1power channels=(1)';
DSSText.command='Export monitors PV_PV1power';
DSSText.Command='export meter';
Metert=xlsread('MasterIEEE37_EXP_METERS.csv');
%%
DSSText.Command='plot monitor object=REG1_Taps';
DSSText.Command='plot monitor object=REG2_Taps';
DSSText.Command='plot monitor object=REG3_Taps';
DSSText.Command='plot monitor object=REG4_Taps';
DSSText.Command='plot monitor object=REG5_Taps';
DSSText.Command='plot monitor object=REG6_Taps';
DSSText.Command='plot monitor object=CAP4_Taps';
DSSText.Command='plot monitor object=CAP5_Taps';
%% xx
DSSText.Command='plot monitor object=Cap1_power';
DSSText.Command='plot monitor object=Cap1_voltage';
DSSText.Command='plot monitor object=Cap2_power';
DSSText.Command='plot monitor object=Cap2_voltage';
DSSText.Command='plot loadshape object=case7';
DSSText.Command='Plot circuit';

```

A.2 OpenDSS Line Codes and Table A.5

```

New linecode.721 nphases=3 BaseFreq=60
!!!~ rmatrix = (0.0554906 | 0.0127467 0.0501597 | 0.00640446 0.0127467 0.0554906)
!!!~ xmatrix = (0.0372331 | -0.00704588 0.0358645 | -0.00796424 -0.00704588 0.0372331)
!!!~ cmatrix = (124.851 | 0 124.851 | 0 0 124.851)
~ rmatrix = [0.055416667 | 0.012746212 0.050113636 | 0.006382576 0.012746212
0.055416667]
~ xmatrix = [0.037367424 | -0.006969697 0.035984848 | -0.007897727 -0.006969697
0.037367424]
~ cmatrix = [80.27484728 | 0 80.27484728 | 0 0 80.27484728]
New linecode.722 nphases=3 BaseFreq=60
!!!~ rmatrix = (0.0902251 | 0.0309584 0.0851482 | 0.0234946 0.0309584 0.0902251)
!!!~ xmatrix = (0.055991 | -0.00646552 0.0504025 | -0.0117669 -0.00646552 0.055991)
!!!~ cmatrix = (93.4896 | 0 93.4896 | 0 0 93.4896)
~ rmatrix = [0.089981061 | 0.030852273 0.085 | 0.023371212 0.030852273 0.089981061]
~ xmatrix = [0.056306818 | -0.006174242 0.050719697 | -0.011496212 -0.006174242
0.056306818]
~ cmatrix = [64.2184109 | 0 64.2184109 | 0 0 64.2184109]
New linecode.723 nphases=3 BaseFreq=60
!!!~ rmatrix = (0.247572 | 0.0947678 0.249104 | 0.0893782 0.0947678 0.247572)
!!!~ xmatrix = (0.126339 | 0.0390337 0.118816 | 0.0279344 0.0390337 0.126339)
!!!~ cmatrix = (58.108 | 0 58.108 | 0 0 58.108)

```


~ rmatrix = [0.245 | 0.092253788 0.246628788 | 0.086837121 0.092253788 0.245]
 ~ xmatrix = [0.127140152 | 0.039981061 0.119810606 | 0.028806818 0.039981061
 0.127140152]
 ~ cmatrix = [37.5977112 | 0 37.5977112 | 0 0 37.5977112]
 New linecode.724 nphases=3 BaseFreq=60
 !!!~ rmatrix = (0.399883 | 0.101765 0.402011 | 0.0965199 0.101765 0.399883)
 !!!~ xmatrix = (0.146325 | 0.0510963 0.139305 | 0.0395402 0.0510963 0.146325)
 !!!~ cmatrix = (46.9685 | 0 46.9685 | 0 0 46.9685)
 ~ rmatrix = [0.396818182 | 0.098560606 0.399015152 | 0.093295455 0.098560606
 0.396818182]
 ~ xmatrix = [0.146931818 | 0.051856061 0.140113636 | 0.040208333 0.051856061
 0.146931818]
 ~cmatrix = [30.26701029 | 0 30.26701029 | 0 0 30.26701029]

Table A.5 for primary feeder sizing [1]

TABLE A.5
Characteristics of Aluminum Cable, Steel Reinforced (Aluminum Company of America)

Circular Mils or AWG Aluminum	Aluminum			Steel			Copper Equivalent ^a Circular Mils or AWG	Ultimate Strength (lb)	Weight (lb/mi)	Geometric Mean Radius at 60 Cycles (ft)	Approx. Current Carrying Capacity ^b (amps)	<i>r_s</i> Resistance	
	Strands	Layers	Strand Diameter (in.)	Strands	Strand Diameter (in.)	Outside Diameter (in.)						25°C (77°F)	
												DC	25 Cycles
1,590,000	54	3	0.1716	19	0.1030	1.545	1,000,000	56,000	10,777	0.0520	1380	0.0587	0.0588
1,510,500	54	3	0.1673	19	0.1004	1.506	950,000	53,200	10,237	0.0507	1340	0.0618	0.0619
1,431,000	54	3	0.1628	19	0.0977	1.465	900,000	50,400	9,699	0.0493	1300	0.0652	0.0653
1,351,000	54	3	0.1582	19	0.0949	1.424	850,000	47,600	9,160	0.0479	1250	0.0691	0.0692
1,272,000	54	3	0.1535	19	0.0921	1.382	800,000	44,800	8,621	0.0465	1200	0.0734	0.0735
1,192,500	54	3	0.1486	19	0.0892	1.338	750,000	43,100	8,082	0.0450	1160	0.0783	0.0784
1,113,000	54	3	0.1436	19	0.0862	1.293	700,000	40,200	7,544	0.0435	1110	0.0839	0.0840
1,033,500	54	3	0.1384	7	0.1384	1.246	650,000	37,100	7,019	0.0420	1060	0.0903	0.0905
954,000	54	3	0.1329	7	0.1329	1.196	600,000	34,200	6,479	0.0403	1010	0.0979	0.0980
900,000	54	3	0.1291	7	0.1291	1.162	566,000	32,300	6,112	0.0391	970	0.104	0.104
874,500	54	3	0.1273	7	0.1273	1.146	550,000	31,400	5,940	0.0386	950	0.107	0.107
795,000	54	3	0.1214	7	0.1214	1.093	500,000	28,500	5,399	0.0368	900	0.117	0.118
795,000	26	2	0.1749	7	0.1360	1.108	500,000	31,200	5,770	0.0375	900	0.117	0.117
795,000	30	2	0.1628	19	0.0977	1.140	500,000	38,400	6,517	0.0393	910	0.117	0.117
715,500	54	3	0.1151	7	0.1151	1.036	450,000	26,300	4,859	0.0349	830	0.131	0.131
715,500	26	2	0.1659	7	0.1290	1.051	450,000	28,100	5,193	0.0355	840	0.131	0.131
715,500	30	2	0.1544	19	0.0926	1.081	450,000	34,600	5,865	0.0372	840	0.131	0.131
666,600	54	3	0.1111	7	0.1111	1.000	419,000	24,500	4,527	0.0337	800	0.140	0.140
636,000	54	3	0.1085	7	0.1085	0.977	400,000	23,600	4,319	0.0329	770	0.147	0.147
636,000	26	2	0.1564	7	0.1216	0.990	400,000	25,000	4,616	0.0335	780	0.147	0.147
636,000	30	2	0.1456	19	0.0874	1.019	400,000	31,500	5,213	0.0351	780	0.147	0.147
605,000	54	3	0.1059	7	0.1059	0.953	380,500	22,500	4,109	0.0321	750	0.154	0.155
605,000	26	2	0.1525	7	0.1186	0.966	380,500	24,100	4,391	0.0327	760	0.154	0.154
556,500	26	2	0.1463	7	0.1138	0.927	350,000	22,400	4,039	0.0313	730	0.168	0.168
556,500	30	2	0.1362	7	0.1362	0.953	350,000	27,200	4,588	0.0328	730	0.168	0.168
500,000	30	2	0.1291	7	0.1291	0.904	314,500	24,400	4,122	0.0311	690	0.187	0.187
477,000	26	2	0.1355	7	0.1054	0.858	300,000	19,430	3,462	0.0290	670	0.196	0.196
477,000	30	2	0.1261	7	0.1261	0.883	300,000	23,300	3,933	0.0304	670	0.196	0.196
397,500	26	2	0.1236	7	0.0961	0.783	250,000	16,190	2,885	0.0265	590	0.235	
397,500	30	2	0.1151	7	0.1151	0.806	250,000	19,980	3,277	0.0278	600	0.235	Same
336,400	26	2	0.1138	7	0.0885	0.721	4/0	14,050	2,442	0.0244	530	0.278	
336,400	30	2	0.1059	7	0.1059	0.741	4/0	17,040	2,774	0.0255	530	0.278	
300,000	26	2	0.1074	7	0.0835	0.680	188,700	12,650	2,178	0.0230	490	0.311	
300,000	30	2	0.1000	7	0.1000	0.700	188,700	15,430	2,473	0.0241	500	0.311	
266,800	26	2	0.1013	7	0.0788	0.642	3/0	11,250	1,936	0.0217	460	0.350	
For Current													
Approx.													
75%													
Capacity^c													
266,800	6	1	0.2109	7	0.0703	0.633	3/0	9,645	1,802	0.00684	460	0.351	0.351
4/0	6	1	0.1878	1	0.1878	0.563	2/0	8,420	1,542	0.00814	340	0.441	0.442
3/0	6	1	0.1672	1	0.1672	0.502	1/0	6,675	1,223	0.00600	300	0.556	0.557
2/0	6	1	0.1490	1	0.1490	0.447	1	5,345	970	0.00510	270	0.702	0.702
1/0	6	1	0.1327	1	0.1327	0.398	2	4,280	769	0.00446	230	0.885	0.885
1	6	1	0.1182	1	0.1182	0.355	3	3,480	610	0.00418	200	1.12	1.12
2	6	1	0.1052	1	0.1052	0.316	4	2,790	484	0.00418	180	1.41	1.41
2	7	1	0.0974	1	0.1299	0.325	4	3,525	566	0.00504	180	1.41	1.41
3	6	1	0.0937	1	0.0937	0.281	5	2,250	384	0.00430	160	1.78	1.78
4	6	1	0.0834	1	0.0834	0.250	6	1,830	304	0.00437	140	2.24	2.24
4	7	1	0.0772	1	0.1029	0.257	6	2,288	356	0.00452	140	2.24	2.24
5	6	1	0.0743	1	0.0743	0.223	7	1,460	241	0.00416	120	2.82	2.82
6	6	1	0.0661	1	0.0661	0.198	8	1,170	191	0.00394	100	3.56	3.56

A.3 Load Model Script

New Load.S701a Bus1=701.1.2 Phases=1 Conn=Delta Model=1 kV= 13.8 kW=190 kVAR=
160

New Load.S701b Bus1=701.2.3 Phases=1 Conn=Delta Model=1 kV= 13.8 kW= 223 kVAR=
170

New Load.S701c Bus1=701.3.1 Phases=1 Conn=Delta Model=1 kV= 13.8 kW= 200 kVAR=
189

New Load.S712c Bus1=712.3.1 Phases=1 Conn=Delta Model=1 kV= 13.8 kW= 189 kVAR=
128

New Load.S713c Bus1=713.3.1 Phases=1 Conn=Delta Model=1 kV= 13.8 kW= 231 kVAR=
199

New Load.S714a Bus1=714.1.2 Phases=1 Conn=Delta Model=4 kV= 13.8 kW= 230 kVAR=
203

New Load.S714b Bus1=714.2.3 Phases=1 Conn=Delta Model=4 kV= 13.8 kW= 183 kVAR=
143

New Load.S718a Bus1=718.1.2 Phases=1 Conn=Delta Model=2 kV= 13.8 kW= 105 kVAR=
89

New Load.S720c Bus1=720.3.1 Phases=1 Conn=Delta Model=1 kV= 13.8 kW= 185 kVAR=
163

New Load.S722b Bus1=722.2.3 Phases=1 Conn=Delta Model=4 kV= 13.8 kW= 207 kVAR=
185

New Load.S722c Bus1=722.3.1 Phases=1 Conn=Delta Model=4 kV= 13.8 kW= 565 kVAR=
352

New Load.S724b Bus1=724.2.3 Phases=1 Conn=Delta Model=2 kV= 13.8 kW= 200 kVAR=
117

New Load.S725b Bus1=725.2.3 Phases=1 Conn= Delta Model=1 kV=13.8 kW= 192 kVAR=
151

New Load.S727c Bus1=727.3.1 Phases=1 Conn=Delta Model=1 kV= 13.8 kW= 214 kVAR=
153

New Load.S728 Bus1=728 Phases=3 Conn=Delta Model=1 kV= 13.8 kW= 193 kVAR=
160

New Load.S729a Bus1=729.1.2 Phases=1 Conn=Delta Model=4 kV= 13.8 kW= 224 kVAR=
154

New Load.S730c Bus1=730.3.1 Phases=1 Conn=Delta Model=2 kV= 13.8 kW= 200 kVAR=
162

New Load.S731b Bus1=731.2.3 Phases=1 Conn=Delta Model=2 kV= 13.8 kW= 205 kVAR=
130

New Load.S732c Bus1=732.3.1 Phases=1 Conn=Delta Model=1 kV= 13.8 kW= 201 kVAR=
176

New Load.S733a Bus1=733.1.2 Phases=1 Conn=Delta Model=4 kV= 13.8 kW= 197 kVAR=
125

New Load.S734c Bus1=734.3.1 Phases=1 Conn=Delta Model=1 kV= 13.8 kW= 205 kVAR=
176

New Load.S735c Bus1=735.3.1 Phases=1 Conn=Delta Model=1 kV= 13.8 kW= 185 kVAR=
125

New Load.S736b Bus1=736.2.3 Phases=1 Conn=Delta Model=2 kV= 13.8 kW= 186 kVAR=
 133
 New Load.S737a Bus1=737.1.2 Phases=1 Conn=Delta Model=4 kV= 13.8 kW= 285 kVAR=
 233
 New Load.S738a Bus1=738.1.2 Phases=1 Conn=Delta Model=1 kV= 13.8 kW= 213 kVAR=
 193
 New Load.S740c Bus1=740.3.1 Phases=1 Conn=Delta Model=1 kV= 13.8 kW= 175 kVAR=
 194
 New Load.S741c Bus1=741.3.1 Phases=1 Conn=Delta Model=4 kV= 13.8 kW=213 kVAR=
 190
 New Load.S742a Bus1=742.1.2 Phases=1 Conn=Delta Model=2 kV= 13.8 kW=212 kVAR=
 176
 New Load.S742b Bus1=742.2.3 Phases=1 Conn=Delta Model=2 kV= 13.8 kW=198 kVAR=
 181
 New Load.S744a Bus1=744.1.2 Phases=1 Conn=Delta Model=1 kV= 13.8 kW=201 kVAR=
 176
 New Load.S700 Bus1=799r Phases=3 Conn=Delta Model=1 kV= 13.8 kW=5700 kVAR=
 1100

A.4 OpenDSS Capacitor Bank Models

! FIXED CAPACITORS

New Capacitor.C703 Bus1=711 Phases=3 Numsteps=3 kVAR=150 kV=13.8 states=[1]

! SWITCHED CAPACITORS

New Capacitor.C730 Bus1=714 Phases=3 Numsteps=3 kVAR=300 kV=13.8

New Capacitor.C711 Bus1=722 Phases=3 Numsteps=3 kVAR=300 kV=13.8

New Capacitor.C737 Bus1=742 Phases=3 Numsteps=3 kVAR=300 kV=13.8

New CapControl.C1ctrl1 element=line. L1 terminal=1 Capacitor=C730 Type=kvr CTratio=1
 ONsetting=600 Offsetting=100 enabled=yes Delay=30 deadtime=300

New CapControl.C1ctrl2 element=line. L1 terminal=1
 Capacitor=C711 Type=kvr CTratio=1 ONsetting=600 OFFsetting=100 enabled=yes Delay=30
 deadtime=300

New Capcontrol.Clctr13 element=line. L1 terminal=1 Capacitor=C737 Type=Kvr CTratio=1
 ONsetting=600 OFFsetting=100 enabled=yes Delay=30 deadtime=300

A.5 Single-phase PV Inverter Code

! PV model

New loadshape.MyIrrad npts=4032 sinterval=300 mult=(file='Enrel_pvout14.txt')
action=normalize

! Bus 701

New PVSystem.PV1 phases=1 bus1=701.1 kV=7.967 kVA=360 irradi=1 %cutin=0.05
%cutout=0.05 Pmpp=360 Daily=MyIrrad PF=0.95

!Bus 713

New PVSystem.PV5 phases=1 bus1=713.2 kV=7.967 kVA=240 irradi=1 %cutin=0.05
%cutout=0.05 Pmpp=240 Daily=MyIrrad PF=0.95

!Bus 718

New PVSystem.PV8 phases=1 bus1=718.2 kV=7.967 kVA=90 irradi=1 %cutin=0.05
%cutout=0.05 Pmpp=90 Daily=MyIrrad PF=0.95

!Bus 720

New PVSystem.PV11 phases=1 bus1=720.2 kV=7.967 kVA=120 irradi=1 %cutin=0.05
%cutout=0.05 Pmpp=120 Daily=MyIrrad PF=0.95

New PVSystem.PV12 phases=1 bus1=720.3 kV=7.967 kVA=120 irradi=1 %cutin=0.05
%cutout=0.05 Pmpp=120 Daily=MyIrrad PF=0.95

!Bus 722

New PVSystem.PV13 phases=1 bus1=722.1 kV=7.967 kVA=300 irradi=1 %cutin=0.05
%cutout=0.05 Pmpp=300 Daily=MyIrrad PF=0.95

New PVSystem.PV14 phases=1 bus1=722.2 kV=7.967 kVA=300 irradi=1 %cutin=0.05
%cutout=0.05 Pmpp=300 Daily=MyIrrad PF=0.95

!Bus 725

New PVSystem.PV16 phases=1 bus1=725.1 kV=7.967 kVA=60 irradi=1 %cutin=0.05
%cutout=0.05 Pmpp=60 Daily=MyIrrad PF=0.95

New PVSystem.PV17 phases=1 bus1=725.2 kV=7.967 kVA=60 irradi=1 %cutin=0.05
%cutout=0.05 Pmpp=60 Daily=MyIrrad PF=0.95

New PVSystem.PV18 phases=1 bus1=725.3 kV=7.967 kVA=60 irradi=1 %cutin=0.05
%cutout=0.05 Pmpp=60 Daily=MyIrrad PF=0.95

!Bus 727

New PVSystem.PV19 phases=1 bus1=727.1 kV=7.967 kVA=60 irradi=1 %cutin=0.05
%cutout=0.05 Pmpp=60 Daily=MyIrrad PF=0.95

New PVSystem.PV20 phases=1 bus1=727.2 kV=7.967 kVA=60 irradi=1 %cutin=0.05
%cutout=0.05 Pmpp=60 Daily=MyIrrad PF=0.95

New PVSystem.PV21 phases=1 bus1=727.3 kV=7.967 kVA=60 irradi=1 %cutin=0.05
%cutout=0.05 Pmpp=60 Daily=MyIrrad PF=0.95

!Bus 728

New PVSystem.PV22 phases=3 bus1=728 kV=7.967 kVA=60 irradi=1 %cutin=0.05
%cutout=0.05 Pmpp=60 Daily=MyIrrad PF=0.95

!Bus 729

New PVSystem.PV23 phases=1 bus1=729.1 kV=7.967 kVA=30 irradi=1 %cutin=0.05
%cutout=0.05 Pmpp=30 Daily=MyIrrad PF=0.95

!Bus 730

New PVSystem.PV25 phases=1 bus1=730.1 kV=7.967 kVA=240 irradi=1 %cutin=0.05
%cutout=0.05 Pmpp=240 Daily=MyIrrad PF=0.95

New PVSystem.PV26 phases=1 bus1=730.2 kV=7.967 kVA=240 irradi=1 %cutin=0.05
%cutout=0.05 Pmpp=240 Daily=MyIrrad PF=0.95

New PVSystem.PV27 phases=1 bus1=730.3 kV=7.967 kVA=240 irradi=1 %cutin=0.05
%cutout=0.05 Pmpp=240 Daily=MyIrrad PF=0.95

!Bus 731

New PVSystem.PV28 phases=1 bus1=731.1 kV=7.967 kVA=180 irradi=1 %cutin=0.05
%cutout=0.05 Pmpp=180 Daily=MyIrrad PF=0.95

New PVSystem.PV29 phases=1 bus1=731.2 kV=7.967 kVA=180 irradi=1 %cutin=0.05
%cutout=0.05 Pmpp=180 Daily=MyIrrad PF=0.95

New PVSystem.PV30 phases=1 bus1=731.3 kV=7.967 kVA=180 irradi=1 %cutin=0.05
%cutout=0.05 Pmpp=180 Daily=MyIrrad PF=0.95

!Bus 733

New PVSystem.PV31 phases=1 bus1=733.1 kV=7.967 kVA=180 irradi=1 %cutin=0.05
%cutout=0.05 Pmpp=180 Daily=MyIrrad PF=0.95

New PVSystem.PV32 phases=1 bus1=733.2 kV=7.967 kVA=180 irradi=1 %cutin=0.05
%cutout=0.05 Pmpp=180 Daily=MyIrrad PF=0.95

New PVSystem.PV33 phases=1 bus1=733.3 kV=7.967 kVA=180 irradi=1 %cutin=0.05
%cutout=0.05 Pmpp=180 Daily=MyIrrad PF=0.95

!Bus 734

New PVSystem.PV35 phases=1 bus1=734.2 kV=7.967 kVA=60 irradi=1 %cutin=0.05
%cutout=0.05 Pmpp=60 Daily=MyIrrad PF=0.95

New PVSystem.PV36 phases=1 bus1=734.3 kV=7.967 kVA=60 irradi=1 %cutin=0.05
%cutout=0.05 Pmpp=60 Daily=MyIrrad PF=0.95

!Bus 735

New PVSystem.PV37 phases=1 bus1=735.1 kV=7.967 kVA=90 irradi=1 %cutin=0.05
%cutout=0.05 Pmpp=90 Daily=MyIrrad PF=0.95

!Bus 736

New PVSystem.PV41 phases=1 bus1=736.2 kV=7.967 kVA=60 irradi=1 %cutin=0.05
%cutout=0.05 Pmpp=60 Daily=MyIrrad PF=0.95

! Bus 737

New PVSystem.PV43 phases=1 bus1=737.1 kV=7.967 kVA=240 irradi=1 %cutin=0.05
%cutout=0.05 Pmpp=240 Daily=MyIrrad PF=0.95

New PVSystem.PV44 phases=1 bus1=737.2 kV=7.967 kVA=240 irradi=1 %cutin=0.05
%cutout=0.05 Pmpp=240 Daily=MyIrrad PF=0.95

!Bus 738

New PVSystem.PV46 phases=1 bus1=738.1 kV=7.967 kVA=300 irradi=1 %cutin=0.05
%cutout=0.05 Pmpp=300 Daily=MyIrrad PF=0.95

New PVSystem.PV47 phases=1 bus1=738.2 kV=7.967 kVA=300 irradi=1 %cutin=0.05
%cutout=0.05 Pmpp=300 Daily=MyIrrad PF=0.95

!Bus 740

New PVSystem.PV50 phases=1 bus1=740.2 kV=7.967 kVA=90 irradi=1 %cutin=0.05
%cutout=0.05 Pmpp=90 Daily=MyIrrad PF=0.95

New PVSystem.PV51 phases=1 bus1=740.3 kV=7.967 kVA=90 irradi=1 %cutin=0.05
%cutout=0.05 Pmpp=90 Daily=MyIrrad PF=0.95

!Bus 741

New PVSystem.PV53 phases=1 bus1=741.2 kV=7.967 kVA=60 irradi=1 %cutin=0.05
%cutout=0.05 Pmpp=60 Daily=MyIrrad PF=0.95

New PVSystem.PV54 phases=1 bus1=741.3 kV=7.967 kVA=60 irradi=1 %cutin=0.05
%cutout=0.05 Pmpp=60 Daily=MyIrrad PF=0.95

!Bus 744

New PVSystem.PV57 phases=1 bus1=744.3 kV=7.967 kVA=60 irrads=1 %cutin=0.05
%cutout=0.05 Pmpp=60 Daily=MyIrrad PF=0.95

! VOLT/VAR

//New XYCurve.vv_curve npts=4 XArray=(0.5,0.95,1.03,1.5) Yarray=(1,1,-1.0,-1.0)
//New InvControl.InvPVCtrl mode=VOLTVAR voltage_curvex_ref=rated
vvc_curve1=vv_curve
//Eventlog=yes

!DYNAMIC REACTIVE CURRENT FUNCTION

//New InvControl.InvTestPVCtrl mode=DYNAMICREACCURR DbVMin=0.97
DbVMax=0.985
//~ ArGraLowV=10.0 ArGraHiV=10.0 DynReacavgwindowlen=120s EventLog=yes

A.6 References

1. Gonen, T. (2014). Electric Power Distribution Engineering (3rd ed.). CRC Press.
<https://doi.org/10.1201/b16455>

APPENDIX B

TYPHOON HIL INITIALIZATION SCRIPTS

The Python Typhoon HIL initialization scripts are written below for the selected case studies. This Appendix contains utility feeder's 1 and 2, transmission line code segments, load scripts, capacitor bank scripts.

B.1 Typhoon HIL Initialization Scripts

```
Texe = 120e-6
# base parameters for calculation
Sn = 20e3
Vn = 13.8e3
Vdc = 400
Ib = Sn / Vn
Zb = Vn**2/Sn
fb = 60
# system parameters
w = 2*np.pi*fb
fsw = 20e3
wsw = 2*np.pi*fsw
Cdc = 18.8e-2
# grid parameters
Lm = 1.75e-5
Rm = 0.000103
# filter calculations
r = 0.2
wres = 0.7*wsw
deltaIImax = 0.01*Sn*np.sqrt(2)/Vn
Li = Vdc/(16*fsw*deltaIImax)
```



```

Lg = r * Li
Cfilter = (Li+Lg)/(Lg*Li * wres**2)
Rsd = 1/(3* wres *Cfilter)
L0 = 2*np.pi*Li/Zb
Vgrid = 13.8e3
VgridFN = Vgrid #Vgrid/np.sqrt(3)
Rshunt = 0.7e6
fgrid = 60
w = 2 * np.pi * 60
Vhigh = Vgrid
Vlow = 4160.0
# Generator
Vgen = Vgrid/np.sqrt(3)
feet2mile = 0.000189394
# Impedances
R_300 = [[1.3368, 0.2101, 0.2130], [0.2101, 1.3238, 0.2066], [0.2130, 0.2066, 1.3294]]
L_300 = [[1.3343/w, 0.5779/w, 0.5015/w], [0.5779/w, 1.3569/w, 0.4591/w], [0.5015/w,
0.4591/w, 1.3471/w]]

R_301 = [[1.9300, 0.2327, 0.2359], [0.2327, 1.9157, 0.2288], [0.2359, 0.2288, 1.9219]]
L_301 = [[1.4115/w, 0.6442/w, 0.5691/w], [0.6442/w, 1.4281/w, 0.5238/w], [0.5691/w,
0.5238/w, 1.4209/w]]

R_302 = 2.7995
L_302 = 1.4855/w

R_303 = 2.7995
L_303 = 1.4855/w

R_304 = 1.9217

```

$$L_{304} = 1.4212/w$$

Lengths

$$\text{dist}_{800_802} = \text{feet2mile} * 5069$$

$$\text{dist}_{802_806} = \text{feet2mile} * 2112$$

$$\text{dist}_{806_808} = \text{feet2mile} * 1901$$

$$\text{dist}_{808_810} = \text{feet2mile} * 5280$$

$$\text{dist}_{808_812} = \text{feet2mile} * 3168$$

$$\text{dist}_{812_814} = \text{feet2mile} * 422$$

$$\text{dist}_{814_850} = \text{feet2mile} * 4224$$

$$\text{dist}_{816_818} = \text{feet2mile} * 1690$$

$$\text{dist}_{816_824} = \text{feet2mile} * 1267$$

$$\text{dist}_{818_820} = \text{feet2mile} * 1478$$

$$\text{dist}_{820_822} = \text{feet2mile} * 4013$$

$$\text{dist}_{824_826} = \text{feet2mile} * 634$$

$$\text{dist}_{824_828} = \text{feet2mile} * 1690$$

$$\text{dist}_{828_830} = \text{feet2mile} * 1690$$

$$\text{dist}_{830_854} = \text{feet2mile} * 3168$$

$$\text{dist}_{832_858} = \text{feet2mile} * 1690$$

$$\text{dist}_{832_888} = \text{feet2mile} * 3168$$

$$\text{dist}_{834_860} = \text{feet2mile} * 1690$$

$$\text{dist}_{834_842} = \text{feet2mile} * 1056$$

$$\text{dist}_{836_840} = \text{feet2mile} * 6758$$

$$\text{dist}_{836_862} = \text{feet2mile} * 1056$$

$$\text{dist}_{842_844} = \text{feet2mile} * 2746$$

$$\text{dist}_{844_846} = \text{feet2mile} * 2746$$

$$\text{dist}_{846_848} = \text{feet2mile} * 4858$$

$$\text{dist}_{850_816} = \text{feet2mile} * 3168$$

```

dist_852_832 = feet2mile * 1056
dist_854_856 = feet2mile * 2956
dist_854_852 = feet2mile * 3379
dist_858_864 = feet2mile * 3379
dist_858_834 = feet2mile * 2746
dist_860_836 = feet2mile * 2112
dist_862_838 = feet2mile * 2112
dist_888_890 = feet2mile * 1056

```

```
# Spot loads
```

```

def apparent_power_balanced(P, Q):
    s_ph = np.sqrt(P**2 + Q**2)
    return (3 * s_ph), (P/s_ph)

```

```

S_807, pf_807 = apparent_power_balanced(50e3, 240e3)
S_822, pf_822 = apparent_power_balanced(15e3, 15e3)
S_830, pf_830 = apparent_power_balanced(295e3, 390e3)
S_834, pf_834 = apparent_power_balanced(158e3, 194e3)

```

```
# Distributed loads
```

```

def z_ph(P, Q, V, w):
    s_ph = np.sqrt(P**2 + Q**2)
    return (P * (V/s_ph)**2), ((Q/w) * (V/s_ph)**2)

```

```
def distributed_load(P, Q):
```

```

    s = [np.sqrt(P[0]**2 + Q[0]**2), np.sqrt(P[1]**2 + Q[1]**2),
         np.sqrt(P[2]**2 + Q[2]**2)]
    pf = [P[0]/s[0], P[1]/s[1], P[2]/s[2]]

```

```

    return s, pf
#Single Phase loads
R_814a_ph1, L_814a_ph1 = z_ph(3e3, 15e3, VgridFN, w)
R_814c_ph3, L_814c_ph3 = z_ph(5e3, 4e3, VgridFN, w)
R_816_ph3, L_816_ph3 = z_ph(5e3, 5e3, VgridFN, w)
R_817_ph3, L_817_ph3 = z_ph(10e3, 4e3, VgridFN, w)
R_825_ph2, L_825_ph2 = z_ph(9e3, 4e3, VgridFN, w)
R_826_ph1, L_826_ph1 = z_ph(5e3, 3e3, VgridFN, w)
R_829_ph3, L_829_ph3 = z_ph(5e3, 5e3, VgridFN, w)
R_832_ph1, L_832_ph1 = z_ph(6e3, 300e3, VgridFN, w)
R_832b_ph2, L_832b_ph2 = z_ph(5e3, 3e3, VgridFN, w)

#Double phase loads
R_803_ph2, L_803_ph2 = z_ph(10e3, 5e3, VgridFN, w)
R_803_ph3, L_803_ph3 = z_ph(5e3, 4e3, VgridFN, w)
R_812_ph1, L_812_ph1 = z_ph(6e3, 2e3, VgridFN, w)
R_812_ph3, L_812_ph3 = z_ph(10e3, 6e3, VgridFN, w)
# Shunt capacitors
def c_shunt(Q, V, w):
    return (Q/w)/(V**2)
Rc = 0.0001
C_824 = c_shunt(600e3, VgridFN, w)
C_826 = c_shunt(600e3, VgridFN, w)
C_830 = c_shunt(600e3, VgridFN, w)
C_PV = c_shunt(300e3, VgridFN, w)

# Regulator
N1_r1 = 90

```

```
N2_r1 = 4
```

```
Na_r1 = 90
```

```
Nb_r1 = 4
```

```
N1_r2 = 95
```

```
N2_r2 = 2
```

```
N1_r3 = 95
```

```
N2_r3 = 2
```

B.2 Pre-built Scada Panel

```
#Import of sci-kit and pywavelets modules
```

```
from sklearn. neural_network import MLPClassifier
```

```
import sklearn. exceptions
```

```
import pywt
```

```
model_path = hil.get_model_file_path ()
```

```
feat_path = os.path.dirname(os.path.dirname(model_path))
```

```
with open (feat_path+"\\extracted features init.csv", "w") as f:
```

```
    f. write ("")
```

```
with open (feat_path+"\\extracted features.csv", "a") as f:
```

```
    f. write("")
```

```
    # Globals
```

```
islanding_flag = False
```

```
capture_counter = 0
```

```
accuracy = 0
```

```
Loaded = False
```

```

LoadedFlagT = False
LoadedFlagU = False
lock = RLock()
with open(feat_path + "\\ieee 34 node islanding.sav", "rb") as f:
    typhoon_model = pickle.load(f)

Vn = 23900.3
vphase_peak_to_pu = 1 / (np.sqrt(2 / 3.0) * Vn)
t_samp = hil.get_sim_step() # Simulation sampling time
freq_samp = 1/t_samp      # Sampling frequency
decimation = 10
freq_grid = 60           # Grid frequency
N_grid_cycles = 4       # Total grid cycles to be captured
N_samp = int(freq_samp * N_grid_cycles / decimation / freq_grid) # Number of samples to be
captured
if (N_samp % 2) != 0:
    N_samp += 1

# store the widget id
#w_id = "b80ba01c888711eb96841c1bb5b93d80"
#wh = panel.get_widget_by_id(w_id)
hil.set_source_sine_waveform('Vs1', rms=230, frequency=60.0, phase=0.0, harmonics_pu=())
panel_path = os.path.join(SETTINGS_DIR, 'solar panel.ipvx')
hil.set_pv_input_file('Photovoltaic Panel 1', file = panel_path, illumination = 1000.0,
temperature = 25.0)

```